CONFIDENTIAL
SECURITY INFORMATION

UCRL-2069
Chemistry-Transuranic Elements

UNIVERSITY OF CALIFORNIA
Radiation Laboratory

Contract No. W-7405-eng-48

CLASSIFICATION CANCELLED
Date 5-12-53
For the Atomic Energy Commission
William S. Johnson
Chief, Declassification Branch

CHEMISTRY DIVISION QUARTERLY REPORT

September, October, November, 1952

December 31, 1952

CONFIDENTIAL
SECURITY INFORMATION

RESTRICTED DATA

This document contains restricted data as defined in the Atomic Energy Act of 1946. Its transmittal or disclosure of its contents in any manner to an unauthorized person is prohibited.

Berkeley, California

TABLE OF CONTENTS

* Previous Chemistry Quarterly Report, UCRL-1959

Page

II. QUARTERLY PROGRESS REPORT. Project 48B

I. QUARTERLY PROGRESS REPORT. Project 48

A. Nuclear Chemistry

G. T. Seaborg and I. Perlman

Radioactive Decay of At^{210}, At^{211}, and Po^{211}

R. W. Hoff, F. Asaro, P. W. Maguire and S. G. Thompson

The nuclides At^{210} and At^{211} have been produced in bombardments of bismuth with helium ions in the 60-inch cyclotron. A pure sample of At^{211} ($<10^{-4}$ At^{210}) may be volatilized from a bismuth target bombarded with 28 Mev helium ions. Existing data indicate At^{211} decays by both alpha and electron capture decay in the following manner:

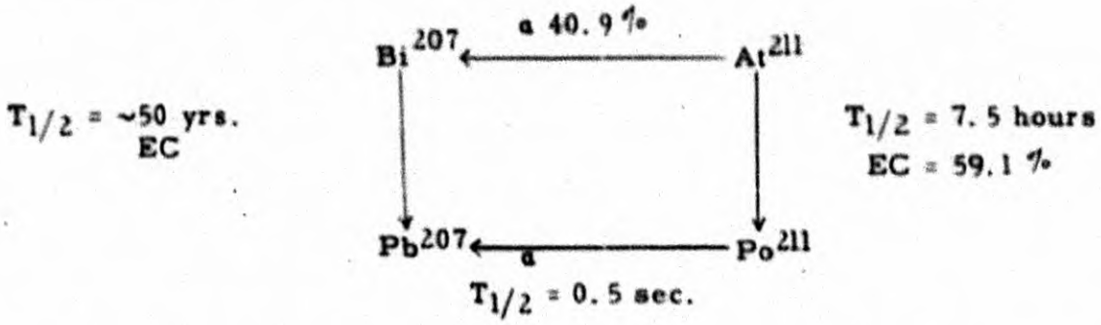

We have searched for γ rays present in the decay of At^{211} using a Na I scintillation spectrometer and have observed no γ rays in appreciable abundance (>1%) besides the K and L X-rays of Po. Therefore, it is reasonable to think that the electron capture decay of At^{211} is directly to the ground state of Po^{211}. There was an indication of very low abundance gamma's in the 540-580 kev region which probably originate from the decay of excited levels of Pb^{207} resulting from the alpha decay of Po^{211}. After the At^{211} activity had decayed to virtually nothing, gamma rays of 540 kev and 880 kev energy were seen from the decay of 50-year Bi^{207}. Although there are numerous gamma rays in the Bi^{207} decay, these were the only two observed due to the small amount of activity present. Previously, the 880 kev level of Pb^{207} has not been detected through conversion electrons of Bi^{207}; however, the level was first seen in the alpha decay of Po^{211}.

A bismuth bombardment using 36 Mev helium ions produces a mixture of At^{211} and At^{210}. In the decay $At^{210} \xrightarrow{EC} Po^{210}$, we have observed gamma rays of 0.250, 1.15, and 1.40 Mev energy. These make the following

energy level diagram for Po^{210} look attractive:

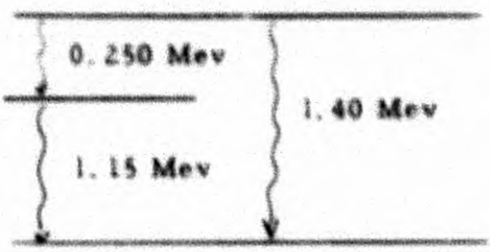

This decay scheme is consistent with the absence of gamma rays in the beta decay of Bi^{210} which has only 1.17 Mev decay energy. Coincidence measurements are being planned to test the correctness of the above decay scheme and also the observation of conversion electrons using a beta-ray spectrometer which will yield, together with scintillation spectrometer data, the amount of decay to each of the excited levels.

A sample containing approximately 5×10^7 d/m of At^{211} has been used to observe the alpha particle energies of Po^{211} in the alpha ray spectrograph. Three low abundance alpha groups of Po^{211} were first reported by Neumann and Perlman, Phys. Rev. 81, 958 (1951). The first two of these groups have been measured with energies 6.881 ± 0.01 Mev and 6.556 ± 0.01 Mev and abundances 0.50 percent and 0.53 percent with respect to the highest group. Work is in progress to find the lowest energy alpha of Po^{211} reported to be 0.1 percent abundant and to have 6.34 Mev energy. Partial scanning of the plate indicates no alpha group between 6.32 and 6.40 Mev which is more than 0.02 percent abundant. Further scanning should decide the actual existence of this third low-intensity group.

The energy of the alpha particles from the decay of At^{211} has been determined with the spectrograph using Am^{241} as an energy standard. The result for At^{211} is 5.862 ± 0.008 Mev.

A large sample of At^{211} containing approximately 4×10^8 alpha dis./min. and approximately an equal amount of At^{210} electron capture activity has yielded interesting results in the alpha ray spectrograph. Three new alpha groups have been seen in the energy region just above Po^{210} with energies 5.355, 5.437, 5.519 ± 0.005 Mev and of approximately equal abundance. A probable fourth group has been seen with energy 5.464 ± 0.01 Mev and in much lower abundance. The origin of these alphas is probably from a very small amount of alpha-branching in the decay of At^{210}, although it is possible that these groups may be of complex structure in the alpha decay of At^{211}. This question will be resolved from a sample of pure At^{211} which has been run on the spectrograph. Assignment of one or more of these alpha energies to At^{210} is consistent with alpha decay systematics in that the nuclide with 125 neutrons has a lower alpha energy than either of its neighboring isotopes. Similar results have been found for the 125 neutron isotopes of Po and Em. Assuming these alphas originate from the decay of At^{210},

one can calculate the abundance of each group. From a consideration of alpha decay theory, it is possible to calculate a hindrance factor for the decay. At^{211} is shown in Table I for comparison:

TABLE I

Isotope	Alpha Particle Energy	Alpha Disintegration Energy	Observed $T_{1/2}$ (hr.)	Alpha Branching Ratio (%)	Alpha $T_{1/2}$ (yrs.)	Hindrance Factor
At^{210}	5.519	5.626	8.3	0.054	1.75	800
At^{210}	5.437	5.543	8.3	0.051	1.85	300
At^{210}	5.355	5.459	8.3	0.062	1.53	100
At^{211}	5.862	5.975	7.5	40.9	19.00	60

Nuclear Properties of Berkelium and Californium Isotopes

E. K. Hulet, A. Ghiorso and S. G. Thompson

In the continuation of the work on the transplutonium isotopes one new isotope of californium has been found and new information concerning berkelium and californium isotopes has been gained. The results have been obtained from a single bombardment with 35 Mev helium ions upon curium and americium.

The target contained ~800 micrograms Cm^{242}, ~40 micrograms Cm^{243}, ~40 micrograms Cm^{244}, ~0.3 micrograms Cm^{245}, ~2 mg. Am^{241}, and ~200 micrograms Am^{243}. The berkelium and californium fractions were individually spearated from all other radioactive elements by the use of ion-exchange methods.

Half-Life for Spontaneous Fission of Cf^{246}

When the logarithm of the known spontaneous fission half-lives of even-even nuclides are plotted as a function of Z^2/A, a straight line is obtained,[1,2] and an extrapolation of this line would predict approximately

1. G. T. Seaborg, Phys. Rev. 85, 157 (1952).
2. W. J. Whitehouse and W. Galbraith, Nature 169, 494 (1952).

2,000 years for the spontaneous fission half-life of Cf^{246}. By counting fission events from a known amount of essentially pure Cf^{246} produced in this bombardment, in a parallel plate ionization chamber, the value found for the spontaneous fission half-life of Cf^{246} was 2100 ± 300 years. This is in excellent agreement with the predicted value. The fission rate decreased with the same 35 hour half-life as that observed for the alpha decay of Cf^{246}, thus proving that the observed fission originated from this isotope.

A New Isotope of Californium

After the nearly complete radioactive decay of Cf^{246} alpha pulse analysis showed some alpha radioactivity, with the energy of 6.24 ± 0.02 Mev, remaining in the californium fraction. It is very likely that these alpha particles originate from Cf^{248} by reasons of yield and alpha systematics considerations. It is very unlikely that Cf^{249} could have been produced in an observable amount, and Cf^{247} would be expected to decay chiefly by an orbital electron capture with a half-life of a few hours. No half-life has been determined for the reasons that the amount of alpha activity is very small, and the period of decay has been short compared with the expected half-life.

Nuclear Properties of Cm^{245}

Previous work at this laboratory yielded an isotope of berkelium believed to have the mass number 245.[3] Radiations from the daughter, Cm^{245}, resulting from the nearly pure electron capture of Bk^{245} have not been previously observed, although its identification in mixtures of curium isotopes by the use of the spectrograph has been made. In this bombardment it was observed that several alpha counts per minute with a particle energy of 5.52 ± 0.05 Mev grew from the berkelium parent. Alpha particles with the above energy were found in a curium fraction chemically separated from pure berkelium after allowing the Bk^{245} to decay for a period of time, and they were also found on a sample plate after nearly complete decay of Bk^{245} originally on the plate. The ratio of the abundance of the new alpha radioactivity to the amount of Bk^{245} that had decayed remained the same in both instances.

The energies of the gamma rays originating from Bk^{245} were measured by a sodium iodide scintillation counter connected to a pulse analyzer. In order of abundances these energies are: 115 kev, 75 kev, and 240 kev. The 115 kev gamma-ray corresponds to the K X-rays of curium which occur after the K orbital electron capture by berkelium. The abundance of the K X-ray was measured, and the same crystal was calibrated at the same geometry with the K X-rays from the K electron capture of At^{211}, for which the K electron capture disintegration rate has been experimentally related to the alpha particle counting rate.[4] From the data obtained it has been possible to calculate a minimum half-life for Cm^{245} of 1,500 years. Any L orbital electron capture by Bk^{245} would increase the half-life of Cm^{245} and a likely upper limit would be 2,800 years.

---

3. Hulet, Thompson, Ghiorso and Street, Phys. Rev. 84, 366 (1951).
4. R. W. Hoff, private communication (October 1952).

Chemistry of the Lanthanide Elements

D. C. Feay and B. B. Cunningham

Because of the similarities between the actinide and lanthanide elements, there has been a continued interest in the lanthanide elements, especially in their nontripositive states, at this laboratory.

Chemistry of Cerium

Cerium tetrafluoride was prepared by the action of elemental fluorine on cerium trifluoride as previously reported.[1]

In order to determine the composition of this compound more accurately than is possible by X-ray diffraction techniques, the loss of weight during the conversion of the tetrafluoride to the dioxide was determined. A weighed sample (about 600 micrograms) of CeF_4 was heated in a tarred platinum crucible at 600° C in air (in a muffle furnace) until the sample attained constant weight. The product was identified by X-ray analysis. Then the actual and theoretical percentage weight losses were compared, and from this the composition of the starting material was calculated. It was assumed that CeO_2 was the only final product. However, Mrs. Carol Dauben of the X-ray group reported that the lattice constants of the CeO_2 were slightly larger than the literature values. This could indicate the presence of oxyfluorides and would also indicate that the original material is purer than calculated from the data in Table 2. Neglecting this factor the average composition of the tetrafluoride is $CeF_{3.98}$.

Attempts were made to determine the thermal stability of CeF_4 by heating it in a nickel effusion vessel for 10 minutes at various temperatures in high vacuum. However, despite pretreatment of the vessel with fluorine from the decomposition of CeF_3, some of the fluorine released from the tetrafluoride reacted with the vessel. Since the amount of fluorine lost by the sample was to be determined by weighing the sample before and after heating, this made our results unreliable for quantitative measurement. This error was detected when the composition of the final product as determined by X-ray analysis and the weight loss method did not agree within any reasonable limit of error. The X-ray analysis indicated that more CeF_4 had been converted to the trifluoride than by the weight loss method. However, our results do show that cerium tetrafluoride is stable in vacuum at 150° C and is decomposed quantitatively to the trifluoride at 230° C.

A spectrographic analysis of the material used for these measurements showed the presence of less than 0.1 percent impurities in the tetrafluoride.

---

1. Cunningham, B. B., D. C. Feay, and M. A. Rollier, UCRL-1632, pp 5-8 (January 28, 1952).

TABLE 2

Composition of CeF_4

Sample	Final Product	Percentage Weight Loss Experimental	Theoretical	Molecular Weight of Sample	Composition of Sample
84	Dioxide	19.90	20.36	214.90	$CeF_{3.94}$
86	"	20.11	20.36	215.46	$CeF_{3.96}$
87	"	20.65	20.36	216.93	$CeF_{4.04}$
Average	"	20.22	20.36	215.76	$CeF_{3.98}$

Chemistry of Terbium

The TbF_4 was prepared by the action of elemental fluorine on the trifluoride as reported previously.[1] The composition of the tetrafluoride was determined in the same manner as was cerium tetrafluoride. The oxide products were identified by comparing the lattice constants of the oxide produced with the curve of the variation of lattice constant with oxygen content of the terbium oxides. The composition selected for the oxide is subject to our experimental error as well as any errors inherent in the published curve.[2]

Also, it was noted that if the sample was heated at about 300° C, TbF_3 is formed. Continued heating at 400°,C produces TbOF. A terbium oxide is produced when the heating is done at about 600° C. The lattice constants of TbOF as determined by X-ray powder diffraction methods for the rhombohedral unit cell are as follows:

$$a = 6.689 \pm 0.007\text{A},$$

$$\alpha = 33.40 \pm 0.10^{\circ}.$$

Since there is no reason to expect the conversion of the tetrafluoride to stop exactly at the tri- or oxyfluoride, the composition of the tetrafluoride was calculated only from the data on the oxides (Table 3). This gives an average composition of $TbF_{3.92}$.

Spectrographic analysis of the sample used in these determinations showed less than 0.1 percent of impurities.

---

2. Gruen, D. M., W. C. Koehler, and J. J. Katz, J. Am. Chem. Soc. 73, 1475-9 (1951).

TABLE 3

Composition of TbF_4

Sample	Temperature	Product	Weight Loss (Percentage) Experimental	Theoretical	Composition
88	400° C	TbOF	16.94	17.43	--
88	600	$TbO_{1.675}$	20.75	20.91	$TbF_{3.97}$
89	320	TbF_3	8.89	8.08	--
89	430	TbOF	16.04	17.43	--
90	215	TbF_3	7.37	8.08	--
90	430	TbOF	17.26	17.43	--
90	600	$TbO_{1.645}$	20.31	21.13	$TbF_{3.87}$
Average					$TbF_{3.92}$

Chemistry of Samarium

The preparation of SmF_4 was attempted by the action of elemental fluorine on SmF_3 at about 350° C for one hour. No tetrafluoride was obtained.

The X-ray work on the fluorides was done by Mrs. Carol Dauben and Mrs. Helena Ruben of Dr. D. H. Templeton's X-ray Diffraction Group.

Isotope Shift in the Spectrum of Plutonium

John G. Conway

Isotope shifts have been measured in the spectrum of plutonium. Two isotopically enriched samples were used, one a mixture of 238-242, the other of 239-240. The samples were loaned for the experiment by Dr. S. G. Thompson. The spectra were photographed on the 35 foot Paschen mounting at the Argonne National Laboratory. Dr. Mark Fred of Argonne is the co-author of a more detailed paper which will appear shortly. A total of 27 lines showed an isotope shift. The four lines exhibiting the greatest shifts are listed in Table 4.

TABLE 4

λ(in A)	Δλ	
	242-238	240-239
3958.79	+0.204	+0.072
3972.06	+0.142	+0.045
3985.37	+0.160	+0.053
4021.41	+0.225	+0.073

Nuclear Emulsion Studies of Alpha Conversion Electron Coincidences in Cf^{246} and Pu^{234}

Dean C. Dunlavey

Complex structure in the alpha decay of a sample of Cf^{246} provided by S. Thompson and K. Hulet and of Pu^{234} in a sample provided by R. Hoff has been observed, using the method of counting alpha-conversion electron coincidences in nuclear emulsions.

Observation of 5100 Cf^{246} alpha events showed 12 percent ± 3 percent to have L or M conversion electrons of 20-25 kev or 35-40 kev energies, indicating an excited level of approximately 43 ± 5 kev in Cm^{242}. For Pu^{234}, only 400 alpha events were counted and 15 percent ± 5 percent of the events were found to have L or M conversion electrons of 25-30 kev or 40-45 kev energies, indicating an excited level of approximately 47 kev in U^{230}. The results are shown in Table 5.

Percentages of decay leading to the excited level are less than expected for each isotope. Explanation, if any is needed, can be that: for Cf^{246}, a few percent of the L conversion electrons might have been missed because of a shorter-than-average track length complicating difficulties of detection already present from the low energy involved; for Pu^{234}, as a result of the small number of events counted, the larger limit of error is enough to include the expected value of nearer 20 percent.

TABLE 5

	Exp alpha $T_{1/2}$	Alpha decay E_{Mev}	Alpha $T_{1/2}$	Preston radii	$r_0 = r/A^{1/3}$	Excited level hindrance $T_{1/2}exp/T_{1/2}$ cal.	Ground state hindrance re CM^{242}
Cf^{246}	35.7h	6.90	49.5h	9.35	1.500		1.08
		6.86	298.0h	8.97		4.76	
Pu^{234}	9.38d	6.34	11.0d	9.34	1.516		0.60
		6.29	62.5d	9.05		3.34	

The Half-Life and Alpha-Particle Energy of Ra^{213}

Floyd Momyer

Attempts were made to find activities belonging to neutron-deficient isotopes of radium by bombarding lead with C^{12} ions and isolating radium samples from the target for alpha pulse analysis.

The lead to be bombarded was affixed to stainless steel plates by cleaning the surface of the plates with a special flux and then melting the lead onto the stainless steel. Such targets were mounted on a probe designed so that the back of the stainless steel plate could be cooled by a continuous flow of water to prevent melting of the lead.

After a 5-10 minute bombardment, the lead was dissolved in a minimum amount of hot 2-3N HNO_3 and the solution cooled in ice and saturated with HCl gas. Barium carrier was then added to precipitate $BaCl_2$ and carry radium, the lead remaining in solution as a chloride complex. The $BaCl_2$ precipitate was washed with cold saturated HCl, dissolved in water and evaporated down on platinum plates for alpha pulse analysis.

In several runs small amounts of a short-lived alpha activity with a 6.9 Mev alpha particle were observed. In one run several hundred counts per minute of this activity were observed on the pulse analyzer and the half-life and alpha-particle energy determined as 2.7 ± 0.3 minutes and 6.90 ± 0.04 Mev, respectively. After decay of this activity several counts per minute of Em^{209} were observed on the plate, free of significant amounts of any other activities. Em^{209} was identified by its measured half-life of about 30 minutes and alpha-particle energy of 6.02 Mev.

From the chemical properties of the new activity and the observance of Em^{209} in samples of it, it is assigned to Ra^{213}. As the half-width of the Ra^{213} peak was almost 300 kev in the best run (due to thickness of the sample), the presence of Fr^{213} from the electron capture decay of Ra^{213} is not at present ruled out. The alpha-particle energies of Ra^{213} and Fr^{213} are probably separated by less than 100 kev.

The Alpha-Branching of AcK and the Presence of Astatine in Nature

E. K. Hyde and A. Ghiorso

Starting with a 20 mc source of Ac^{227} the 21 minute isotope AcK (Fr^{223}) has been isolated and subjected to study to identify its alpha branch products. It has been found that the alpha branching ratio is approximately 4×10^{-5} and that the product isotope, At^{219}, has a 0.9 minute half-life for the emission of 6.27 Mev alpha particles to produce the previously unreported activity Bi^{215}. Bi^{215} is an 8 minute beta emitter. Since Ac^{227} occurs in nature as part of the U^{235} decay chain this establishes the presence of an astatine isotope in a natural source. A complete report of this work is given in UCRL-2019.

Beta Spectrum of Fr^{223}

Thomas O. Passell

Preliminary runs have been made with the double focussing Siegbahn type beta spectrometer to determine the beta spectrum of Fr^{223}. This isotope is a member of the actinium (4n + 3) natural radioactive decay chain. The 21 minute Fr^{223} was milked from a 20 mc source of Ac^{227}, and in a matter of 40-55 minutes from the initial separation the francium was inserted in the spectrometer.

From the Kurie Analysis of the spectrum, there appear to be two components above 450 kev with maximum energies of ~1.0 Mev and ~1.5 Mev, the lower energy component being by far the most abundant. The literature value of 1.2 Mev represents a cloud chamber determination.

Some data have been acquired on the energies of conversion electron lines superimposed upon the beta spectrum and lines resulting from conversion of the three previously reported gamma rays (48.6, 90.0, and 330 kev) have been at least qualitatively confirmed. This study will be continued.

Nucleon Momentum Distributions from High Energy (d,p) Excitation Functions

J. O. Rasmussen, Jr.

It is the purpose of this note to suggest that with certain reasonable assumptions, semi-quantitative information concerning nucleon momentum distributions in nuclei may be gained from the rate of decrease of the (d,p) reaction yield with increasing deuteron energy.

The necessary assumptions are the following:

1. Observed (d,p) reaction yields in the high energy region ($E_d \gtrsim 50$ Mev) are due mainly to the Oppenheimer-Phillips mechanism with the contribution from compound nucleus formation followed by evaporation of a single proton negligible. That is, the observed yield comes from interactions with only the neutron of the deuteron.

2. Coulomb repulsion effects, which largely determine the (d, p) excitation function for low energies, have negligible effect on the high energy slopes of the (d, p) yield curves.

3. The distribution of excitation energies of the residual nucleus (following capture of the neutron from the deuteron) which contribute to the observed (d, p) yield remains essentially the same for all high bombardment energies, and this distribution is quite narrow, peaking near the neutron binding energy. The contribution to the (d, p) yield by states of much lower excitation is expected to be much smaller since the nuclear level density falls off rapidly with decreasing excitation. The contribution by states of much higher excitation energy than the neutron-binding energy is expected to be small on account of the effective competition of neutron evaporation (and in some cases fission) processes with the radiation process.

There are two theoretical treatments from which we shall make quantitative estimates of the bombardment energy dependence of the (d, p) total cross section. A differential (d, p) cross section expression may be obtained from the theoretical work of Chew and Goldberger[1] on the inverse process, the deuteron pick-up process, if we use the principle of detailed balance.[2] Secondly, Daitch and French[3] give a Born approximation derivation of the differential (d, p) cross section and demonstrate the equivalence of their Born approximation formulation with that of Butler.[4]

From the Chew-Goldberger[1] treatment we get the relative differential cross section in their notation as follows, where only factors dependent on incident deuteron and outgoing proton momentum vectors are retained:

$$\frac{d\sigma_{dp}}{d\Omega} \propto \frac{k}{R} \frac{N(\vec{K} - \vec{k})}{\left[\beta^2 + (\vec{k} - \frac{\vec{K}}{2})^2\right]^2} \qquad (1)$$

---

1. Chew and Goldberger, Physical Review 77, 470 (1950).

2. Cf. E. Fermi, Nuclear Physics, University of Chicago Press, p. 146, Eq. VIII.18, 1950.

3. Daitch and French, Physical Review 87, 900 (1952).

4. Butler, S. T., Proc. Roy. Soc. (London) 208, 559 (1951).

where

$\vec{K}$ and $\vec{k}$ are the wave number vectors of the incoming deuteron and outgoing proton, respectively,

K and k are their absolute values,

β is a constant numerically equal to the wave number of a 50 Mev nucleon,

$N(\vec{K}-\vec{k})$ is the momentum probability distribution of the captured neutron in the final nucleus having momentum corresponding to the vector difference $\vec{K}-\vec{k}$,

$d\Omega$ is the element of solid angle.

To obtain the total (d, p) cross section we need to integrate over all angles between $\vec{K}$ and $\vec{k}$ and sum over all final states, weighted according to their relative contributions to the observed (d, p) reaction yield. In this approximate treatment we shall not explicitly perform the summation but will interpret $N(\vec{K}-\vec{k})$ as a momentum distribution averaged over the various contributing final nuclear states. We shall carry out the angular integration for a single average energy of the outgoing proton, for simplicity choosing the proton energy equal to the deuteron energy, the process being capture of the neutron in a nuclear state bound by 2.23 Mev.

If $E_p = E_d$, then $k = \frac{K}{\sqrt{2}}$, and if θ is the angle between $\vec{k}$ and $\vec{K}$,

$$(\vec{K} - \vec{k})^2 = K^2 (3/2 - \sqrt{2}\cos\theta)$$

and (2)

$$(\vec{k} - \frac{\vec{K}}{2})^2 = \frac{K^2}{2} (3/2 - \sqrt{2}\cos\theta).$$

First, the integration will be carried out using a gaussian momentum distribution for $N(\vec{K} - \vec{k})$, since it is analytically convenient and has been successfully applied by Cladis[5] in correlating quasi-elastic proton scattering data. The factor

$$\frac{1}{\left[\beta^2 + (\vec{k} - \frac{\vec{K}}{2})^2\right]^2}$$

will be approximated by the gaussian

$$\exp\left[-\frac{(\vec{k} - \frac{\vec{K}}{2})^2}{\delta^2}\right],$$

5. Cladis, J. B., Ph.D. Thesis (Physics), University of California (1952), issued as U.C. Radiation Laboratory Report No. 1621 (unpublished).

and the choice of δ^2 corresponding to a nucleon energy of 36 Mev gives a good fit over the momentum range of importance.

$$\sigma_{dp} \propto \frac{k}{K} \, 2\pi \int_0^{\pi} \frac{N(\vec{K} - \vec{k})}{\left[\beta^2 + (\vec{k} - \vec{K}/2)\right]^2} \sin\theta \, d\theta \qquad (3)$$

$$\propto \frac{2\pi k}{K} \int_0^{\pi} \exp\left[- \frac{(\vec{K} - \vec{k})^2}{\epsilon^2} - \frac{(\vec{k} - \vec{K}/2)^2}{\delta^2} \right] \sin\theta \, d\theta$$

and with

$$E_p = E_d,$$

k/K is independent of E_d, and we can write

$$\sigma_{dp} \propto \int_0^{\pi} \exp\left[- K^2 \left(\frac{3}{2} - \sqrt{2}\cos\theta\right) \left(\frac{1}{\epsilon^2} + \frac{1}{2\delta^2}\right) \right] \sin\theta \, d\theta$$

Let

$$\frac{1}{\eta^2} = \frac{1}{\epsilon^2} + \frac{1}{2\delta^2} \qquad (4)$$

then

$$\sigma_{dp} \propto \frac{\eta^2}{K^2} \exp\left[- \frac{3}{2} \frac{K^2}{\eta^2} \right] \sinh \sqrt{2} \, \frac{K^2}{\eta^2} \qquad (5)$$

Now δ^2 was chosen to correspond to a nucleon energy of 36 Mev, and for the numerical calculation here ϵ^2 will be taken as corresponding to 16 Mev from the experimental results of Cladis.[5] Then by Eq. 4 η^2 corresponds to 13.1 Mev. That is, $E_\eta = 13.1$ Mev, where E_η is defined by the equation

$$E_\eta = \frac{\hbar^2 \eta^2}{2M},$$

where M is the mass of a nucleon.

The corresponding relation between the energy and wave number of the deuteron is as follows:

$$E_d = \frac{\hbar^2 K^2}{4M},$$

hence

$$\frac{K^2}{\eta^2} = \frac{2 E_d}{E_\eta},$$

and (4) becomes

$$\sigma_{dp} \propto \frac{E_\eta}{2 E_d} \exp\left[-3 E_d/E_\eta\right] \sinh 2\sqrt{2}\, \frac{E_d}{E_\eta} \qquad (5a)$$

For $E_d > E_\eta$ the following approximation is valid:

$$\sinh 2\sqrt{2}\, \frac{E_d}{E_\eta} \approx \frac{1}{2} \exp\left(2\sqrt{2}\, E_d/E_\eta\right)$$

and

$$\sigma_{dp} \propto \frac{E_\eta}{4 E_d} \exp\left[-(3-2\sqrt{2})\, E_d/E_\eta\right] = \frac{E_\eta}{4 E_d} \exp\left[-0.172\, E_d/E_\eta\right]. \qquad (5b)$$

Numerical calculations using Eq. 5b with E_η = 13.1 Mev are given in Table 6 and plotted on Fig. 1.

Secondly, the angular integration of Eq. 3 has been carried out without approximation using the nuclear momentum distribution originally chosen by Chew and Goldberger,[1] namely,

$$N(\vec{K} - \vec{k}) = \left[\gamma^2 + (\vec{K} - \vec{k})^2\right]^{-2},$$

with γ^2 corresponding to a nucleon energy of 18 Mev. The formula resulting from the integration after separation of the integrand into partial fractions is quite lengthy and hence will not be given here. Numerical results using this formular are given in Table 6 and plotted on Fig. 1. (β^2 chosen to correspond to 50 Mev.)

Thirdly, from the Daitch and French[3] treatment we have the differential cross section expression for formation of a single final state

$$\frac{d\sigma_{dp}}{d\Omega} \propto \frac{k}{K} \frac{\left[t^2 + (\vec{K} - \vec{k})^2\right]^2 \left[\int_0^\infty R_\ell(r)\, j_\ell(|\vec{K} - \vec{k}|r)\, r^2\, dr\right]^2}{\left[a^2 + (\vec{k} - \vec{K}/2)^2\right]^2 \left[\beta^2 + (\vec{k} - \vec{K}/2)^2\right]^2} \qquad (6)$$

where t^2 corresponds to the energy by which the captured neutron is bound in the final nucleus and a^2 corresponds to the binding energy of the deuteron, 2.23 Mev. ℓ is the orbital angular momentum quantum number of the captured neutron, r is the radial distance from the center of the nucleus, $R_\ell(r)$ is the radial part of the captured neutron wave function, and $j_\ell(|\vec{K} - \vec{k}|r)$ is the spherical Bessel function of ℓth order.

The integral in Eq. 6 is just the Fourier transform[6] (not normalized) of the wave function

$$\Psi = R_\ell(r)\, P_\ell(\cos\theta).$$

Since the square of the Fourier transform is just the momentum probability distribution, we choose to replace the square of the integral in Eq. 6 by $N(\vec{K} - \vec{k})$, the average momentum distribution over many final states.

---

6. Schiff, L. I., Quantum Mechanics, McGraw-Hill Company, p. 105, Eq. 19.9, 1949.

TABLE 6

Theoretical Relative (d, p) Cross Sections
(Normalized to Unity at 50 Mev)

Deuteron Energy E_d (Mev)	Chew-Goldberger matrix element with gaussian momentum distribution	Chew-Goldberger matrix element with inverse square momentum distribution	Daitch-French matrix element with gaussian momentum distribution
50	1.0	1.0	1.0
75	0.47	0.416	-
100	0.256	0.212	0.279
125	0.147	-	-
150	0.088	0.068	0.100
175	0.056	-	-
200	0.035	0.0326	0.041

Also, since we have chosen to evaluate the integral with $E_p = E_d$, then $t^2 = a^2$. We have the integral

$$\sigma_{dp} \propto 2\pi \frac{k}{K} \int_0^{\pi} \frac{\left[a^2 + K^2 \left(\frac{3}{2} - \sqrt{2}\cos\theta\right)\right]^2}{\left[a^2 + \frac{K^2}{2}\left(\frac{3}{2} - \sqrt{2}\cos\theta\right)\right]^2} \cdot \frac{N\left[K^2\left(\frac{3}{2} - \sqrt{2}\cos\theta\right)\right]}{\left[\beta^2 + \frac{K^2}{2}\left(\frac{3}{2} - \sqrt{2}\cos\theta\right)\right]^2} \sin\theta \, d\theta \quad (7)$$

The integral is the same as that in Eq. 3 with the addition of the new factor in numerator and denominator of the integrand. The new factors nearly compensate one another, their quotient being unity for K = 0 and approaching 4 for large K. For $E_d > 50$ Mev the new factors can be well approximated by

$$\frac{\left[a^2 + Z^2\right]^2}{\left[a^2 + \frac{Z^2}{2}\right]^2} \approx 4\left[1 - 0.6 \exp\left(-\frac{Z^2}{7a^2}\right)\right].$$

Again making the same gaussian approximation for the factor involving β^2 and carrying out the angular integration the final expression is obtained as follows:

$$\sigma_{d,p} \propto \frac{\eta^2}{K^2} \exp\left(-\frac{3}{2}\frac{K^2}{\eta^2}\right) \sinh \sqrt{2}\frac{K^2}{\eta^2} - 0.6 \frac{\eta^2}{K^2} \exp\left(-\frac{3}{2}\frac{K^2}{\zeta^2}\right) \sinh \sqrt{2}\frac{K^2}{\zeta^2}, \quad (8)$$

where

$$\frac{1}{\zeta^2} = \frac{1}{7a^2} + \frac{1}{\eta^2}.$$

E_ζ is defined, analogous to E_η, as

$$E_\zeta = \frac{\hbar^2 \zeta^2}{2M}.$$

Then making the substitutions for K^2, η^2, and ζ^2 as in Eq. 5a and the approximation of the hyperbolic sine as in Eq. 5b, one obtains

$$\sigma_{d,p} \propto \frac{E_\eta}{4E_d} \exp\left[-0.172\, E_d/E_\eta\right] - \frac{0.6\, E_\zeta}{4E_d} \exp\left[-0.172\, E_d/E_\zeta\right]. \quad (8a)$$

Taking E_n, as before, equal to 13.1 Mev and taking E_a = 2.23 Mev, the binding energy of the deuteron, one obtains the value

$$E_\zeta = 7.12 \text{ Mev.}$$

The numerical results from this third formulation are given in Table 6 and Fig. 1.

For comparison with the theory are plotted in Fig. 1 the experimental values for the absolute (d,p) reaction cross sections at high energies for target nuclides, Bi^{209}, Th^{232}, and U^{238}. The Bi cross sections are from the work of Fung,[7] and the Th and U from work of Slater.[8]

In Fig. 1 it is seen that there is little difference between the three theoretical formulations. The agreement of the theoretical slopes with the Bi^{209} results is fortuitously good, but the U and Th curves are much flatter than theoretical. The general agreement is encouraging, but the approximate nature of the formulations must be borne in mind. In the first place the nuclear momentum distributions used are from work on very light elements and from pick-up process and quasi-elastic scattering experiments, where the momentum distribution applies to ground states of nuclei. The interpretation of the distribution $N(\vec{K}-\vec{k})$ used here must be as the average momentum distribution for the captured neutron, an excited nuclear state. The former and the latter distributions should not be expected to be comparable in a quantitative sense.

The significant point set forth by this comparison is that the slope of the high energy (d,p) cross section probably gives a semi-quantitative measure of the momentum distribution of the captured neutron in the excited nuclear state following capture. In this language one would interpret the striking difference between the slope of the Bi^{209} curve, on the one hand, and of the Th^{232} and U^{238} curves, on the other, as indicating a more rapid fall-off of high momentum components in the neutron captured by Bi than in neutrons captured by Th and U. One might speculate that the different Bi behavior is related to the fact that the neutron is the 127th, just following a closed shell. Whether this behavior is a simple consequence of the decreased neutron binding energy or of a more subtle dependence on the form of the nuclear wave function will require data on other nuclides in order to be resolved.

---

7. Fung, S. C., Ph.D. Thesis (Chemistry), University of California (1951), issued as U.C. Radiation Laboratory Report No. 1465 (unpublished), p. 22.

8. Slater, L. M., Unpublished Results.

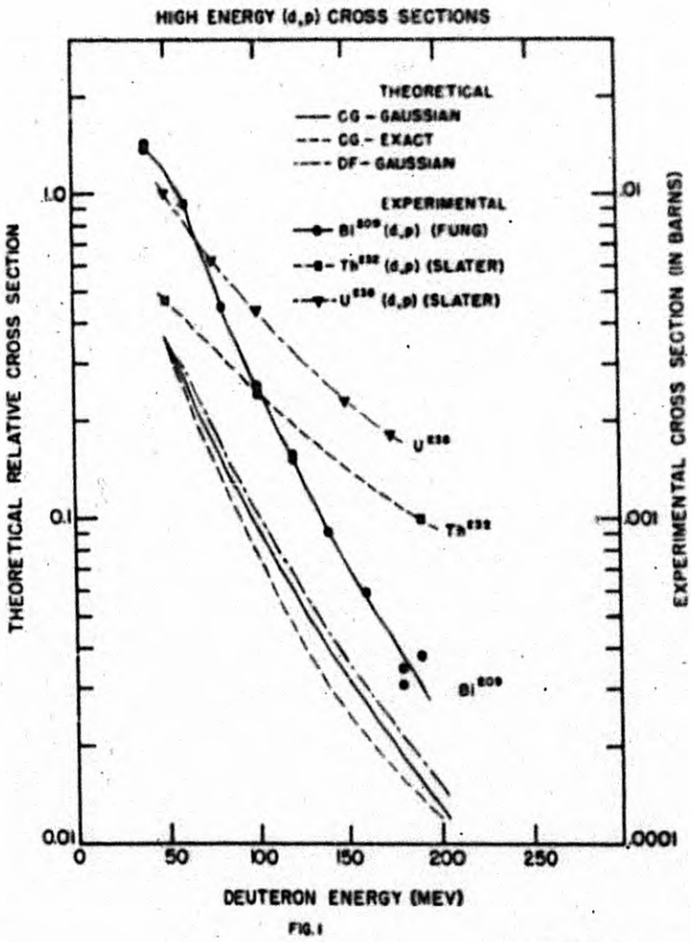
HIGH ENERGY (d,p) CROSS SECTIONS
THEORETICAL
CG - GAUSSIAN
CG - EXACT
DF - GAUSSIAN
EXPERIMENTAL
Bi209 (d,p) (FUNG)
Th232 (d,p) (SLATER)
U238 (d,p) (SLATER)
U238
Th232
Bi209
THEORETICAL RELATIVE CROSS SECTION
EXPERIMENTAL CROSS SECTION (IN BARNS)
1.0
0.1
0.01
.01
.001
.0001
0
50
100
150
200
250
DEUTERON ENERGY (MEV)

FIG. 1

MU-4740

A Report on the Radiochemical Separation of Bismuth from Lead, Polonium and Radium

B. A. Raby and E. K. Hyde

During the course of a study of the alpha branching of the francium isotope, AcK, a need arose for a rapid chemical method for the isolation of Bi^{215} from a solution containing amounts of francium, lead, and radium radioactivity many-fold greater. Since Bi^{215} has the short half-life of eight minutes and the alpha branching of AcK which gives rise to Bi^{215} (via the intermediate activity, At^{219}) is very slight (10^{-4} to 10^{-5}), the chemical separation of Bi^{215} from its contaminants must be rapid and thorough. The bothersome contaminants which occur in this particular decay scheme are Fr^{223}, Ra^{223}, Bi^{211}, and Pb^{211}. The following report summarizes the work done during the last quarter on rapid radiochemical procedures for purification of bismuth in the carrier-free state. The methods studied should prove to be of general applicability and are described in some detail. No claim to originality of these methods is made, but published information is scanty, particularly on anion exchange, and our results may be useful to others.

Anion Exchange

The first of the three methods discussed herein is the use of Dowex-A-1 anion exchange resin; this technique depends on the formation of poly-chloro ions of the elements in question in hydrochloric acid solution.

A column 7 mm. long by 2 mm. in diameter was packed with coarse grains of Dowex A-1. With the aid of suction, solutions were flowed through this column at the rate of about 1 ml. per minute. Using Bi^{210} as a tracer, various conditions of adsorption and desorption were tried. In order to observe their behavior, Ra^{226}, Po^{210}, and Pb^{211} tracer solutions were also run through the column under comparable conditions.

In the extraction of Fr^{223} from Ac^{227}, silicotungstic acid is used.[1] It was found that unless the silicotungstic acid is removed before the bismuth-containing solution is passed through the column, a 70 to 75 percent loss of bismuth occurs at the adsorption stage. This indicates some complexing of bismuth by the silicotungstate ion. Hence the anion exchange method was inapplicable to the problem without a preliminary step, such as those discussed later.

Behavior of Bismuth. The behavior of bismuth on the resin is summarized in Table 7. In all cases, 5µl of tracer containing RaD, E, F, was added to 1.0 ml. of hydrochloric acid solution before adsorption on the resin. The beta activity was counted on shelf two of a standard Geiger-Müller counter

---

1. E. K. Hyde and A. Ghiorso, UCRL-2019.

with an 11.6 mg. aluminum absorber on shelf one to cut out the RaF alpha particles and the soft beta particles of RaD. The observed count in 5 µl of tracer was 1.54×10^5 c/m. The alpha counting rate was 8.0×10^4 c/m.

Desorption was made by elution with 2 ml. of the reagent.

TABLE 7

Anion Exchange Behavior of Bismuth

Composition of Initial Tracer Solution Passed Through A-1 Column	Percent Bismuth Adsorbed	Desorbtion Reagents	Percent Bismuth Desorbed by 2 ml. of reagent
0.1 M - HCL	99	H_2O	0
3 M - HCL	96 - 99	0.1 N - HCL	0
6 M - HCL	95 - 99	4 N - $HClO_4$	0
8 M - HCL	33	conc. HCL	63
10 M - HCL	19	sat. HCL*	72 - 93
		conc. HNO_3	94 - 99

* Made by passing dry hydrogen chloride gas through concentrated hydrochloric acid at 0° C.

Table 7 indicates that adsorption of bismuth is complete from 0.1 M HCL to 6 M HCL and that saturated HCL or concentrated HNO_3 are good desorption agents.

Behavior of Lead. A private communication from H. E. Hicks and P. C. Stevenson revealed to us that Pb(II) in hydrochloric acid solutions adsorbs strongly on anion exchange resins from HCL solutions of a certain concentration range but desorbs readily if the HCL concentration is lower or higher than this range. This behavior was studied for Dowex A-1 in the experiments below.

Thirty-six minute Pb^{211} was used as a tracer and was prepared in the following manner: First 11.2 day Ra^{223} was isolated from a sample of Ac^{227}. Ammonia gas was passed into a dilute HCL solution of the Ac^{227} to which 2 mg. Fe(III) had been added. The $Fe(OH)_3$ precipitate carrying Ra^{223} was dissolved and reprecipitated with NH_3. It was then dissolved in a small amount of HNO_3, a few milligrams of Ba(II) carrier was added, and $Ba(NO_3)_2$ was precipitated by the addition of 10 ml. of cold fuming nitric acid. This precipitation was repeated. The final $Ba(NO_3)_2$ (with which the Ra^{223} had co-precipitated was dissolved in water. One mg. of Bi(III) chloride was added and precipitated as $Bi(OH)_3$ by the addition of

NH_3. This precipitate carried tracer Pb^{211} and separated it from the Ra^{223}. The supernatant solution containing Ra^{223} was acidified (to prevent adsorption of CO_2) and set aside for later reuse as a source of Pb^{211}. The $Bi(OH)_3$ was dissolved, reprecipitated with NH_3 and finally dissolved in HCL.

An aliquot of the Pb^{211} tracer solution was diluted to form 0.5 ml. of solution of the composition shown in the first column of Table 8 below. This solution was passed through a 7 mm. long x 2 mm. in diameter column of Dowex A-1 resin at a flow rate of about 1 ml. per minute. The percentage of the lead passing through the column was determined by alpha counting (of Bi^{211} which came to equilibrium with the Pb^{211} within a few minutes). This percentage is shown in column two. The column was then rinsed with one ml. of hydrochloric acid of the same composition; amount of Pb^{211} desorbed is shown in column three. Then two more ml. of solution were passed through the column; column four shows the amount of Pb desorbed.

TABLE 8

Anion Exchange Behavior of Pb Tracer

Concentration of HCL solutions	Percent Pb not Adsorbed from Initial Solution	Percent Pb Desorbed by first (1 ml.) wash	Percent Pb Desorbed by 2nd (2 ml.) wash
3.0	3.0	89.0	11
4.0	0.4	0.6	~0
4.5	0.4	0.6	~0
5.0	0.5	0.9	~0
5.5	0.6	0.03	~0
6.0	0.8	0.5	~0
6.5	0.9	0.6	~0
7.0	0.6	0.3	~0
7.5	0.6	0.02	~0
8.5	65.0	23.0	~0

An inspection of Table 8 shows that Pb tracer is adsorbed and held strongly by Dowex A-1 resin from hydrochloric acid solutions in the concentration range 4 M to 7.5 M. Below and above this concentration range it can be washed completely from the resin. Comparison with Table 7 indicates that a clean separation of lead and bismuth tracers is readily made by passage of a 1-2 M HCL solution through a short column of Dowex A-1.

Behavior of Polonium. Tompkins[2] has published an ion-exchange study of polonium in which negative chloro-complexes are discussed. Orth[3] has made preliminary studies of adsorption of polonium on Dowex A-1. In the present work, a series of experiments were carried out in HCL and HNO_3 systems using RaF tracer and Dowex A-1 resin.

2. E. R. Tompkins, UCRL-1294.
3. D. Orth, private communication.

In one experiment RaDEF tracer in 2 M HCL was passed through a 7 x 2 mm. column. The column was rinsed in turn with 3 ml. concentrated HCL, and three 1 ml. portions of concentrated nitric acid. Assay of the solutions for RaF alpha activity and RaE beta activity gave the result shown in Table 9.

TABLE 9

Percent Tracer in Solution Passed Through 7 x 2 mm. Column

	Initial 1 ml. 2 M HCL	3 ml. conc. HCL Rinse	First 1 ml. conc. HNO_3	Second 1 ml. conc. HNO_3	Third 1 ml. conc. HNO_3	Total Recovery
Po	5.0	1.3	32.0	41.0	1.4	81 ± 5
Bi	0.5	92.6	3.3	0.1	0.1	97 ± 5

The polonium material balance in the above experiment is only 80 ± 5 percent and the missing 20 percent is ascribed to hydrolyzed and/or polymerized species present in the RaDEF solution which were adsorbed on the resin and not readily desorbed. This difficulty was taken care of in succeeding experiments by utilizing the results of Table 9 to prepare polonium tracer, i.e., the original RaDEF mixture adjusted to 2 M HCL was passed through the resin column, the resin was rinsed with 2 ml. concentrated HCL, and the unhydrolyzed polonium was then desorbed with nitric acid. This polonium solution was evaporated to dryness and taken up in concentrated hydrochloric acid.

Using some of the freshly prepared polonium tracer, the experiment, whose results were given in Table 9, was repeated using a clean resin column. The results are given in Table 10.

TABLE 10

Percent Po Tracer in Solutions
Passed Through 7 x 2 mm. Dowex A-1 Column

1 ml. initial 2 M HCL	2 ml. conc. HCL	First 1 ml. conc. HNO_3	Second 1 ml. conc. HNO_3	Third 1 ml. conc. HNO_3	Total Recovery
7.8	2.8	18.6	66.6	4.6	100 ± 5

Recommended Lead-Bismuth-Polonium Separation Method. The results of the experiments described above, as well as others not mentioned, can be used to formulate an excellent radiochemical separation method for these elements. In outline, a suitable procedure might be:

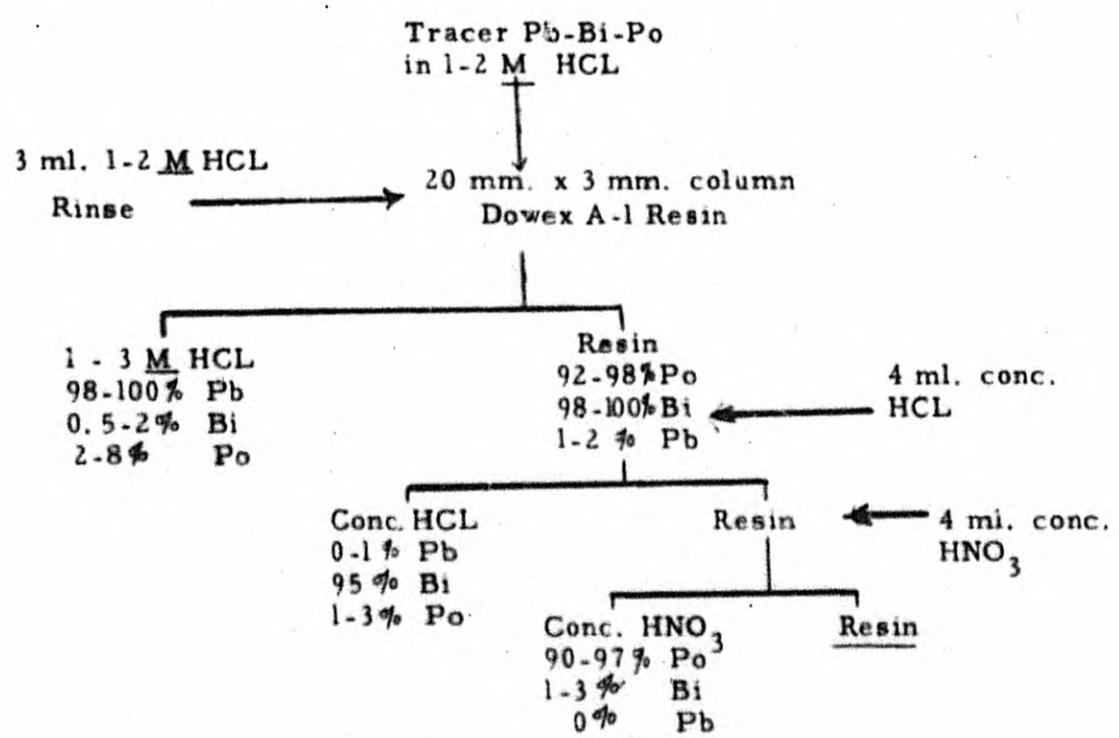

The advantage of this method over those published previously (as for example, for the purpose of preparing RaE and RaF sources) is its simplicity and the fact that all three elements are obtained in a carrier-free state. The separation factors shown in the scheme are conservative and a closer study of conditions, particularly of flow rate and column length, should make it possible to raise them to considerably higher values.

Co-Precipitation of Bi and Pb on MnO_2

It was decided that the co-precipitation of tracer bismuth on MnO_2 might be a useful method of separating Bi^{215} from a solution containing Ack, Ra^{223}, Pb^{211}, and inert silicotungstic acid. The following test runs were run, using RaDEF tracer: $KMnO_4$ was added to a 1 ml. solution of RaDEF tracer to which Ra^{226} tracer, two drops of 0.4 M silicotungstic acid, and 2 mg. Mn(II) salt had been added. After the precipitation of MnO_2 had occurred, the supernate was drawn off and assayed. Carrying of Bi was 90-99 percent, of Ra, 2-6 percent. It was concluded that the MnO_2 method would be a good means to separate bismuth from a silicotungstic acid solution.

Some experiments on the co-precipitation of lead as a function of H^+ concentration were run, using Pb^{211} tracer. One to two mg. of Mn^{++} in 1 ml. of nitric acid solutions of Pb^{211} was precipitated as MnO_2 by the addition of $KMnO_4$, and the activity precipitate was determined. Results are shown in Table 11.

TABLE 11

Co-precipitation of Lead with MnO_2

HNO_3 Concentration	Percent Co-precipitated
~0 M HNO_3	47
1 M HNO_3	10
4 M HNO_3	7

Adsorption of Radiocolloidal Bismuth on Filter Paper

Gile, Garrison and Hamilton[4] have reported an excellent method for the separation of $Bi^{204-206}$ in a carrier-free state from bombarded lead targets. The lead target is dissolved in nitric acid, evaporated to dryness and taken up in 10 percent sodium hydroxide. The lead is converted to soluble $PbO_2^=$, and the bismuth becomes radiocolloidal and is quantitatively adsorbed by passage of the solution through filter paper. The bismuth is then eluted with dilute acid.

An attempt was made to adapt this method to our Bi^{215} isolation problem with particular emphasis on shortening the time. Various preliminary experiments were run to determine the adsorption behavior of bismuth tracer from alkaline solutions on filter paper, glass wool, and other materials in the absence of macroquantities of $PbO_2^=$ ion. These results were erratic and unsatisfactory.

A satisfactory method was developed when $AlO_2^=$ ion was added to the solutions. Five µl RaDEF tracer was added to 300 µl 1 M $Al(NO_3)_3$, and 1 ml 10 percent NaOH was added to form radiocolloidal bismuth in the presence of $AlO_2^=$ ion. The solution was sucked through a one millimeter-thick bed of Whatman No. 50 filter paper pulp supported on a 10 mm. coarse sintered disc. The adsorbed Bi^{210} tracer was washed with 2 ml. 10 percent sodium hydroxide and with 2 ml. distilled water (to remove NaOH). The bismuth was then desorbed with 300 µl concentrated hydrochloric acid to form a carrier-free solution. This procedure took only 8 - 10 minutes and recovery was about 90 percent. RaF contamination was about 5 percent. In check runs with Ra^{226} tracer, about 1 percent of the radium was found in the final bismuth fraction. Similar check runs with Pb^{211} tracer showed 1 percent contamination of the bismuth fraction with lead.

---

4. Gile, Garrison and Hamilton, UCRL-1017.

Application of above Methods to a Branching of AcK

Several combinations of these three methods, i.e., MnO_2 precipitation, Dowex A-1 anion exchange method, and the radiocolloidal adsorption on filter paper, were used in attempts to isolate 8 minute Bi^{215} from AcK (Fr^{223}), which in turn was separated from a 20 mc. source of Ac^{227}. In every case the results were negative, but nevertheless they were useful in setting an upper limit of 10^{-4} to the a branching of Fr^{223}.

Extraction Behavior of Trivalent Lanthanides and Actinides Elements into Tributyl Phosphate from Hydrochloric and Nitric Acids

P. R. Gray and S. G. Thompson

Recently, D. F. Peppard P. R. Gray, and G. W. Mason[1] at the Argonne National Laboratory studied the extraction characteristics of La, Ce, Pm, Eu, Ac, Pu, Am, and Cm into tributyl phosphate from concentrated hydrochloric and nitric acids, 12.0 N and 15.6 N respectively. Their data, when plotted as the logarithm of the distribution ratio (the ratio of the concentration of the element in the tributyl phosphate phase to the concentration in the acid phase) against the atomic number of the element, gives a straight line in all instances.

As a contribution to the chemistry of berkelium and californium, it seemed of interest to study their extraction behavior under the conditions used by Peppard et al., to determine if the straight line functions still existed. Bk and Cf tracers were obtained from K. Hulet of this laboratory.

The results are illustrated by the lower curves of Figs. 2 and 3; the data for Ac, Pu, Am, and Cm being that of Peppard et al., with the exception that Ac in the HNO_3 was redetermined, the distribution ratio agreeing quite favorably with the previous result. It is seen that in HNO_3, Bk and Cf show no marked deviation from the continuation of the straight line previously found. However, in HCl, both Bk and Cf have ratios which are factors of at least five greater than would be predicted from the previous data.

It seemed expedient to study further the lanthanide elements for a similar effect, since Peppard's data is only for La (57), Ce (58), Pm (61), and Eu (63), while Tb (65) would be the analogue to Bk (97). Er (69), Tm (70), and Yb (71) tracers were obtained from the Argonne National Laboratory through the courtesy of L. Glendennin and E. Steinberg. Tb (65) tracer and inactive Ho (66) were available in this laboratory.

---

1. Work to be published in a coming issue of the J. Phys. Chem.

The results for these elements are illustrated by the upper curves of Figs. 2 and 3 as a continuation of Peppard's data.

It can be seen that a straight line results from the HNO_3 data while a marked deviation occurs again in HCl, occurring not at Tb (65) but at Er (68). It is to be noted that the actinide data in HCl has been shifted from its usual position with Ac and La as analogues in order to show the similarity of their behavior in HCl.

At the present time, the nature of this deviation in behavior in HCl is being investigated.

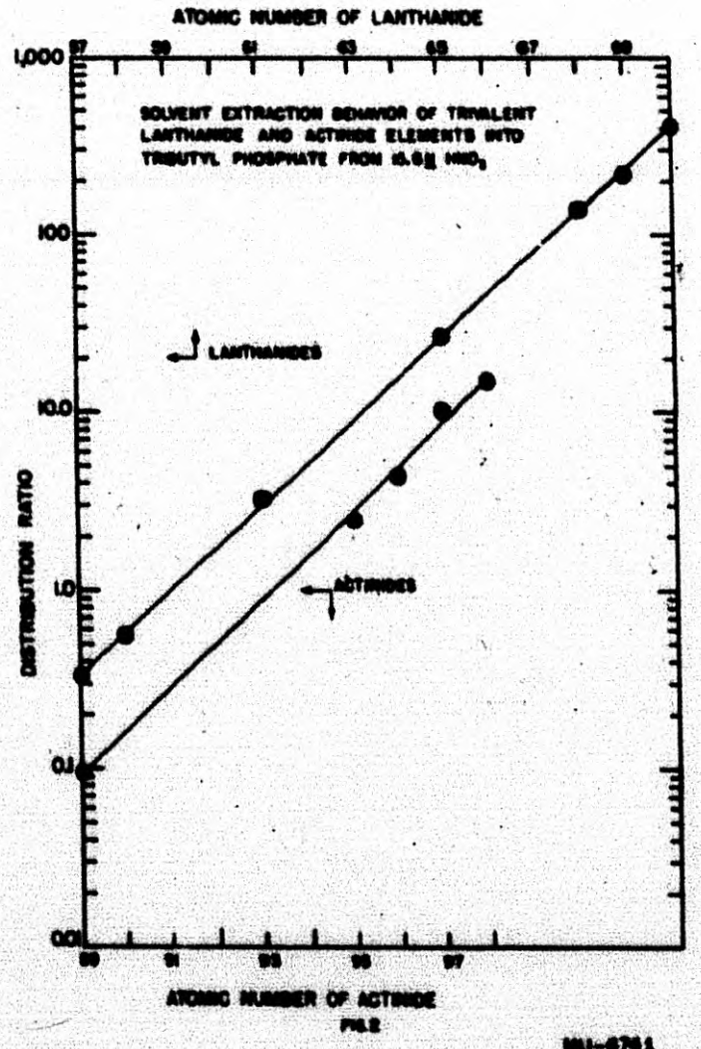
ATOMIC NUMBER OF LANTHANIDE
SOLVENT EXTRACTION BEHAVIOR OF TRIVALENT LANTHANIDE AND ACTINIDE ELEMENTS INTO TRIBUTYL PHOSPHATE FROM 15.6M HNO3
LANTHANIDES
ACTINIDES
DISTRIBUTION RATIO
1,000
100
10.0
1.0
0.1
0.01
ATOMIC NUMBER OF ACTINIDE
MU-6761

FIG.2

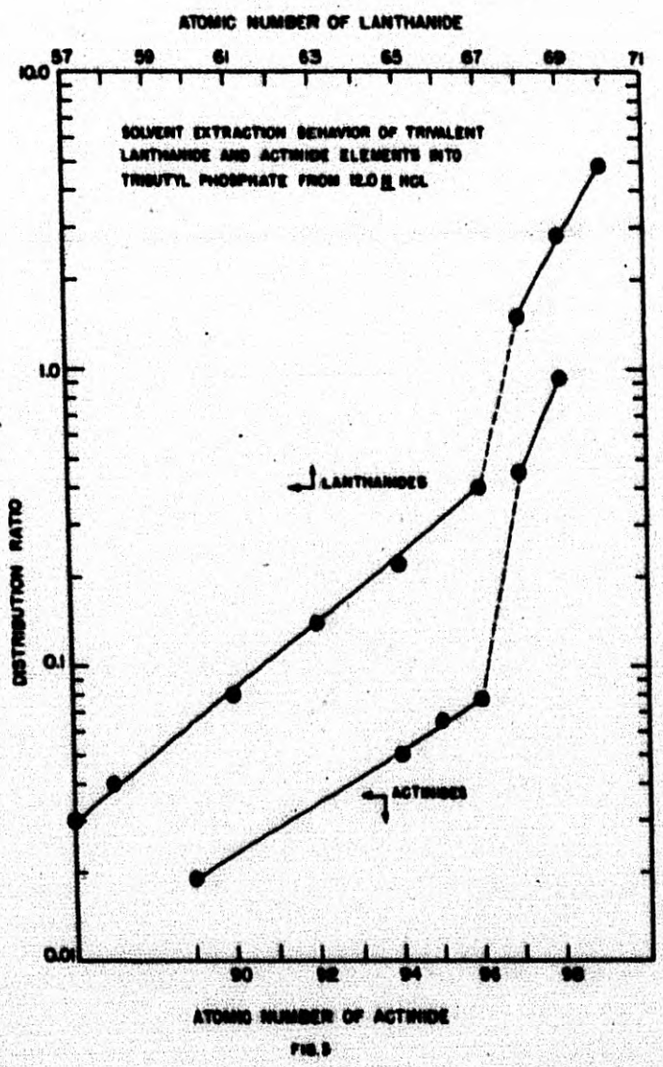
ATOMIC NUMBER OF LANTHANIDE
57
59
61
63
65
67
69
71
10.0
1.0
0.1
0.01
SOLVENT EXTRACTION BEHAVIOR OF TRIVALENT LANTHANIDE AND ACTINIDE ELEMENTS INTO TRIBUTYL PHOSPHATE FROM 12.0 M HCl
LANTHANIDES
ACTINIDES
DISTRIBUTION RATIO
90
92
94
96
98
ATOMIC NUMBER OF ACTINIDE

FIG. 9

MU-4762

Saturation Backscattering Correction for Windowless Proportional Counter with 2π Geometry

Dwight Conway and John Rasmussen

In order to use the Mark 12 Nucleometer chamber[1] (windowless proportional counter) for absolute beta counting, the saturation backscattering correction is needed. This was studied using methane at atmospheric pressure as the counting gas. The backing materials used were lead, brass, aluminum, beryllium, and polystyrene. A hard and a soft beta emitter (with no gamma radiation) were used: (1) a mixture of Sr^{90}-Y^{90} in equilibrium (E_{max} = 0.61 and 2.2 Mev, respectively) and (2) Pm^{147} (E_{max} = 0.223 Mev). The samples were mounted on thin tygon films made conducting with thin films of silver and counted in 4π proportional counter of the type developed by Borkowski[2] to determine the absolute disintegration rate and then in the 2π counter to obtain the backscattering correction.

The method of calculating the backscattering coefficient is as follows: let y equal the counting rate in the 2π counter, x equal that in the 4π counter, and z equal that on the sample side of the film (i.e., counts recorded in only one-half of 4π counter chamber) in the 4π counter for a particular sample. The calculation of the backscattering coefficient, B, the fraction of beta particles starting into the backing material which are scattered out into the counting volume, is straightforward, if scattering end absorption by the tygon and silver films for sample mounting are negligible. That is,

$$B = (y - 0.5\,x)/0.5\,x$$

The assumption of negligible scattering and absorption by the mounting was verified in the case of the hard beta sample (Sr^{90}-Y^{90}) by a second method, namely, the backscattering correction was determined for Sr^{90}-Y^{90} also by depositing directly on polystyrene, covered with a conducting layer of carbon, and on lead and aluminum 50 γ aliquots from a solution whose specific activity was determined in the 4π counter. The thickness of each of these samples was about 0.25 mg/cm^2, whereas that of the corresponding film sample was about 0.5 mg/cm^2. The corrections as determined by the methods using tygon film and by depositing directly on the backing are essentially the same (Cf Fig. 4).

In the case of the soft Pm^{147} radiation, the scattering and absorption by the mounting film is not negligible, as evidenced by the fact that the counting rate of the sample film with activity up was higher than when the film was activity side down.

---

1. Radiation Counter Laboratories, Skokie, Illinois.
2. "Report of Conference on Absolute Beta Counting," National Research Council (February 28, 1949).

An attempt was made to correct the data for the effect of the mounting film in order to calculate a backscattering factor to compare with Sr^{90}-Y^{90} results. That is, for the Pm^{147} results it was assumed that

$$B = (y-z)/(x-z).$$

The Pm^{147} results should be checked as were the others by mounting the sample directly on the backing.

The backscattering factors determined in this investigation are plotted against the atomic number of the backscattering material in Fig. 4. Also plotted for comparison are the data of Zumwalt[3] for the saturation backscattering of Co^{60} (E_{max} = 0.31 Mev) at 2π geometry. There is a considerable discrepancy between his and our results for the lighter elements. These differences might be due to such causes as differences in the threshold electron energy necessary to produce a count.

Noteworthy is the fact that for large Z, the 2π geometry backscattering factor is noticeably lower than for a 3 percent of 4π geometry, thus indicating the anisotropy of backscattered radiation with preferential scattering in a direction perpendicular to the backing plate. This anisotropy has been pointed out previously by Yaffe.[4] It is to be expected that the self-scattering, self-absorption correction will also be different for 2π than for lower geometries.

---

3. L. R. Zumwalt from "Report of Conference on Absolute Beta Counting," National Research Council (February 28, 1949), page 23.
4. L. Yaffe from "Report of Conference on Absolute Beta Counting," National Research Council (February 28, 1949), page 27.

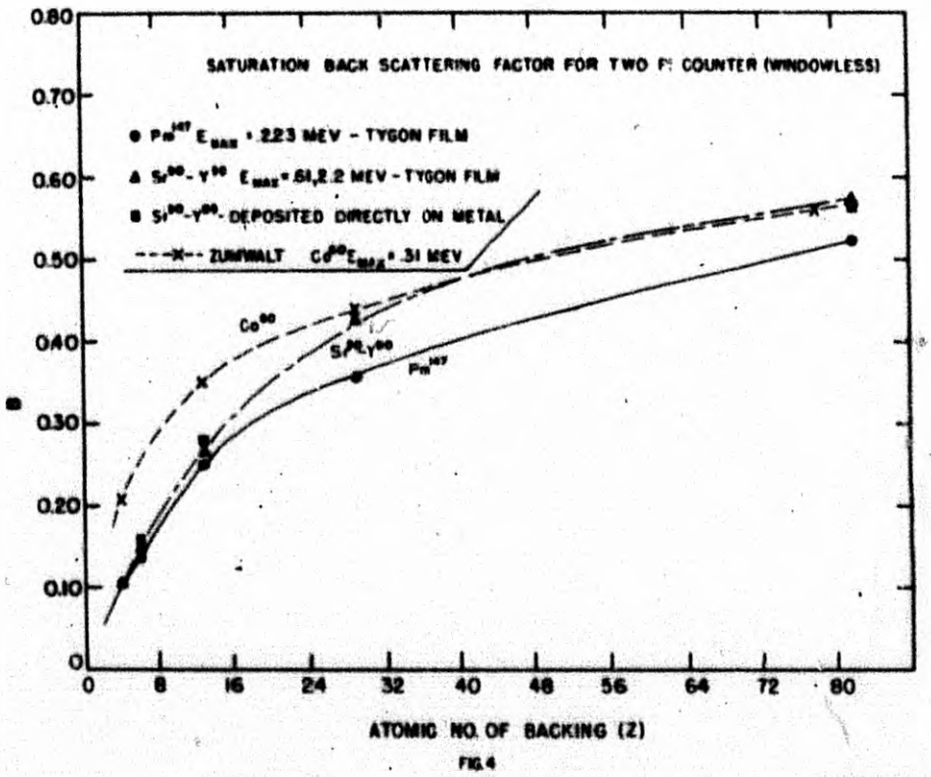
SATURATION BACK SCATTERING FACTOR FOR TWO PI COUNTER (WINDOWLESS)
● Pm^{147} E_{MAX} = .223 MEV - TYGON FILM
▲ Sr^{90}-Y^{90} E_{MAX} = .61,2.2 MEV - TYGON FILM
■ Sr^{90}-Y^{90} - DEPOSITED DIRECTLY ON METAL
---x-- ZUMWALT Co^{60} E_{MAX} = .31 MEV
Co^{60}
$Sr^{90}Y^{90}$
Pm^{147}
m
0.80
0.70
0.60
0.50
0.40
0.30
0.20
0.10
0
0
8
16
24
32
40
48
56
64
72
80
ATOMIC NO. OF BACKING (Z)

FIG. 4

MU-4743

B. Bio-Organic Chemistry

M. Calvin and A. A. Benson

Synthesis of High Specific Activity D, L-Leucine-3-C^{14}

R. Ostwald

The synthesis of high specific activity D, L-leucine-3-C^{14} has been carried out using a procedure described in some detail for other compounds in our Quarterly Report for September, October and November, 1951. The procedure consists of the following steps: (1) The potassium salt of acetamidomalonate is condensed with isobutyl iodide-1-C^{14} by refluxing for six hours in an evacuated bomb tube in the presence of tertiary butanol and potassium tertiary butoxide, followed by removal of the solid potassium iodide and evaporation of the solution to dryness. (2) The condensation product is hydrolyzed by refluxing with concentrated hydrochloric acid for 76 hours. (3) The amino acid mixture is separated and purified on a Dowex 50 ion exchange column.

By means of this procedure, three separate amino acid preparations were carried out using 11.2, 12.1 and 5.0 mc. of isobutyl iodide-1-C^{14}. The crude amino acid mixtures contained 6.7, 6.6 and 2.1 mc. respectively, representing 60 percent, 54 percent and 42 percent of the starting activity. The separation on ion exchange columns, as described below, showed that the amino acid mixture consisted of leucine, glycine, α-aminobutyric acid, alanine (approximately 0.2 percent of the crude amino acid activity), and a radioactive ninhydrin-negative compound appearing near leucine (R_F values slightly greater than those for leucine) in a two-dimensional descending paper chromatogram developed with phenol-water and butanol-propionic acid-water. This compound contained about 8 percent of the radioactivity of the crude amino acid product.

The purification of the crude amino acid mixture was performed on 590 cc. Dowex 50 cation exchange resin (250-500 mesh) in a glass column 2.5 cm. in diameter and 120 cm. long. The capacity of the column was 1770 meq., the amino acid load was 56 meq. (17.6 mc.) representing 3.2 percent of the resin capacity. After the sample had been applied the column was washed with 6 ℓ of water; this effluent contained 2.2 μc. The amino acids were then eluted with 1.03 N HCl at a flow-rate of 15 cc./hour or 0.05 cm./min. Every fifth fraction (approximately 15 cc. per fraction) was analyzed by applying an aliquot portion to paper, counting the spot and then chromatographing with butanol-propionic acid-water solvent.

(a) From 0-1600 cc. acid (0.93 times column capacity expressed in meq. acid) came 0.65 μc. consisting of only trace amounts of glycine and other amino acids.

(b) From 1600-2930 cc. acid (0.93-1.70 times column capacity) came 4 μc., consisting of inactive glycine and radioactive alanine and leucine, containing 75 percent and 17 percent respectively of the radioactivity in this fraction.

(c) From 2930-3355 cc. acid (1.70-1.95 column capacity) came 0.6 μc. consisting of radioactive α-aminobutyric acid, leucine, and an unknown, ninhydrin-negative compound containing 70 percent, 25 percent and 5 percent respectively of the radioactivity in this fraction.

(d) From 3355-4865 cc. acid (1.95-2.85 times column capacity) came 1.3 mc. consisting of radioactive leucine and an unknown containing 92 percent and 9 percent respectively of the radioactivity in this fraction, together with traces of radioactive valine.

(e) From 4865-8575 cc. acid (2.85-5.03 times column capacity) came 15.2 mc. consisting of radioactive leucine and an unknown containing 97 percent and 3 percent respectively of the radioactivity in this fraction.

Purification of the leucine by recrystallization from water, after boiling with charcoal, removed the unknown compound.

The total yield of D,L-leucine hydrochloride was 2.958 g. (66 percent of theoretical) with a specific activity of 5.6 μc./mg. (theoretical = 6.7 μc./mg). The yield on a radioactivity basis is 16.5 mc. (59 percent of theoretical). The recovery of radioactivity from the ion exchange column was quantitative.

Synthesis of Glycine-2-C^{14} and Aspartic Acid-3-C^{14}

R. Noller

Glycine-2-C^{14}

Glycine-2-C^{14} hydrochloride (6.62 μc./mg), containing no radioactive impurities, has been prepared from sodium acetate-2-C^{14} by reacting ammonia with chloroacetic acid. The yield was 67 percent based on the starting sodium acetate.

A small quantity of impurity was isolated from the crude glycine having a specific activity corresponding to the compound, imino-diacetic-2-C_2^{14}-acid·HCl.

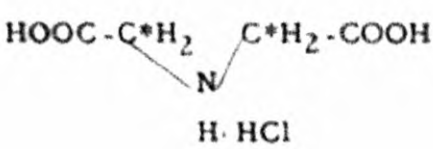

Aspartic Acid-3-C^{14}

Aspartic-3-C^{14} acid·HCl (5.7 μc./mg.) has been prepared from sodium acetate-2-C^{14} via the condensation of ethylchloroacetate-2-C^{14} with diethylacetamidomalonate (see Quarterly Report for April, May, June 1951).

It has been found that most amino acids prepared by condensing organic halides with diethylacetamidomalonate followed by hydrolysis of the product are contaminated with other radioactive compounds. The best way to obtain a pure product is to fractionate the mixture by means of an ion exchange column. In seeking to avoid the difficulties involved in the use of an ion exchange column, it was found that the aspartic acid product could also be purified through the preparation of its copper salt.

To this end, the crude hydrolysate was dissolved in a small quantity of water and transferred to a beaker. Copper chloride (7.67 g. $CuCl_2 \cdot 2H_2O$, 4/3 molar excess over theoretical total amino acid yield) was then added to the hydrolysate solution and the total volume brought to 150 ml. This solution was then titrated (with stirring) to pH 5, using about 97 ml. of 1 N sodium hydroxide. The solution was then placed in the refrigerator for at least two days.

Approximately 4 ml. of "Celite Analytical Filter Aid" (Johns Manville) was then added to the cold solution. The solution was filtered through a 0.25 cm. bed of "Celite" and the precipitate washed with ice water until the filtrate was chloride free. The precipitate was then redispersed in about 150 ml. water, about 0.5 ml. concentrated hydrochloric acid added, and hydrogen sulfide gas bubbled through the solution with stirring for 2-1/2 hours. The solution was heated on a steam bath for 15 minutes and then allowed to cool to room temperature with continuous stirring. It was filtered through a 0.5 cm. bed of "Celite" which was then rinsed with slightly acid water (1 ml. concentrated hydrochloric acid in 200 ml. water) until most of the activity was removed.

Concentrated hydrochloric acid (25 ml.) was added to the filtrate which was then evaporated to dryness on a steam bath. The aspartic acid hydrochloride was dissolved in a mixture of 25 ml. concentrated hydrochloric acid and 25 ml. water and again dried. It was then redissolved in a small quantity of water, treated with activated charcoal, and filtered into a tared sample container, and the solution evaporated to dryness.

Two dimensional paper chromatography showed that there were no amino acids other than aspartic acid, and that there was less than 1 percent of a radioactive impurity which may have been a chromatographic anomaly.

The yield of aspartic-3-C^{14} acid HCl was 2190 g., 5.7 μc./mg., 66 percent based on starting activity. The theoretical specific activity was 5.6 μc./mg.

Aspartic-4-C^{14} acid HCl has been prepared in similar yields by starting with carboxyl labeled sodium acetate.

Studies in Morphine Metabolism

H. Rapoport and C. H. Lovell

Two paths are being investigated for the preparation of codeine- and morphine-1-C^{14}. The first method, outlined in our previous report, has progressed through the periodate oxidation:

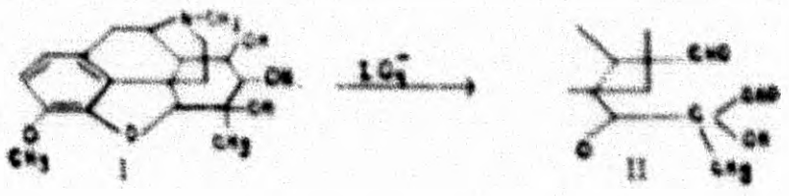

I II

Only one mole of periodate was consumed per mole of triol to give a product stable toward further oxidation. For this reason, lead tetraacetate oxidation of the triol is now under examination.

The second path, which has the advantage of introducing the radioactivity at a very late stage in the synthesis, is outlined below:

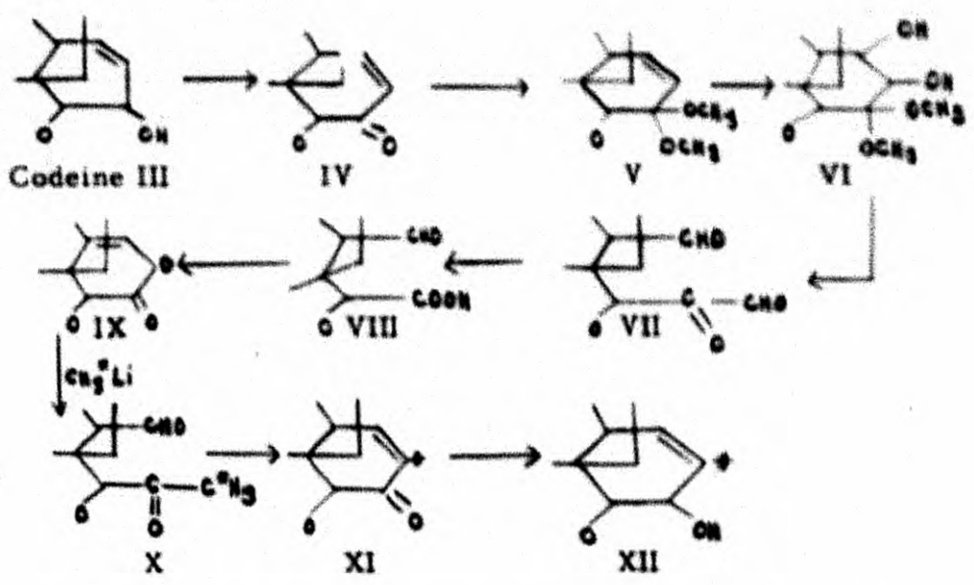

Codeine III IV V VI VII VIII IX X XI XII

Work on this reaction has progressed successfully through the ketal V.

Effect of Heparin on the Rate of Metabolism of Fatty Acids and Other Compounds

M. Kirk and A. Hughes

Rate of Appearance of $C^{14}O_2$ in the Breath

The investigation of the effect of heparin on fatty acid metabolism in rats has continued, with the emphasis being placed on acetate metabolism. Also, the effect of heparin on some other types of compounds has been studied. In the last Quarterly Report, it was stated that the heparin apparently facilitated the metabolism of fatty acids to carbon dioxide. Repetition of the experiments with acetate, however, indicates that the "heparin effect" is quite variable or non-existent. It will be noted, however, that the greatest variation is with the "control" animals, rather than with those receiving heparin.

Experimental. The same general procedure has been used which was previously outlined. Modifications included: 1) changes in total weight of acetate injected, but without change in the amount of radioactivity used. 2) use of animals which have been starved for 24 hours, and 3) use of crystalline heparin (Connaught Laboratories) dissolved in distilled water instead of heparin solution (Upjohn). Compounds tested included: Sodium acetate-2-C^{14}, alanine-1-C^{14}, alanine-2-C^{14}, alanine-3-C^{14}, sodium lactate-3-C^{14} and choline-n-methyl-C^{14}.

Results. There has been found no significant difference between the metabolism of fatty acids with or without heparin. The choline results represent only one experiment. Table 12 gives the values for the compounds tested.

Conclusions. The potentiation of fatty acid metabolism by heparin is questionable. More detailed investigation into the dietary condition of the animals is necessary to ascertain whether there has been any significant change in the diet which might be causing the disappearance of the "heparin effect".

The effect of heparin on the metabolism of choline should be further studied. Not only is the total recovery enormously different from that of the other compounds studied, but the slope of the rate curve is significantly different also.

Appearance of Radioactivity in Various Blood Components

To expand the investigation of a method by which heparin may be able to affect fatty acid metabolism, experiments are being conducted to determine the amount of labeling of various components of blood from rats injected with sodium acetate-2-C^{14}, with and without heparin.

TABLE 12

Compound	No. of Experiments	Without heparin: Total % of activity recovered 3 hrs.	Av.	7 hrs.	Av.	With heparin: Total % of activity recovered 3 hrs.	Av.	7 hrs.	Av.
Acetate-2-C^{14} 2 mg. - Fed Animals.	4	78.92		91.26		83.16		93.45	
		73.31		83.40		80.53		90.27	
		80.80	78.29	90.29	88.80	71.48	77.83	81.91	88.33
		77.03		86.89		79.66		90.58	
		80.34		92.54		78.21		88.14	
		75.35		88.39		73.95		35.67	
Acetate-2-C^{14} 20 mg. - Fed Animals	4	76.21		86.73		77.18		87.54	
		45.32		56.04		82.22		90.87	
		66.93	65.18	77.96	75.70	74.81	81.71	84.66	91.59
		72.24		82.86		92.61		103.27	
Acetate-2-C^{14} 20 mg. -Starved Animals	8	84.75		98.59		84.74		97.34	
		78.32		88.72		72.04		83.63	
		80.55		89.72		82.11		94.15	
		80.27	83.44	88.82	94.52	82.71	79.44	94.89	90.81
		86.21		95.88		74.90		85.59	
		82.68		94.12		71.66		80.64	
		83.42		96.72		82.93		94.76	
		91.34		103.62		84.40		95.25	
Alanine-1-C^{14} Starved Animals	3	77.98		90.56		86.83		98.99	
		89.53	84.80	102.07	96.64	80.52	82.19	93.36	94.06
		86.90		97.32		79.23		89.84	
Alanine-2-C^{14} Starved Animals	4	56.33		76.83		53.75		72.89	
		49.88	51.22	69.69	72.72	52.41	49.49	72.35	68.25
		45.61		70.53		40.94		57.30	
		53.06		73.83		50.85		70.45	
Alanine-3-C^{14} Starved Animals	3	45.27		65.34		38.04		54.82	
		44.01	44.80	64.01	65.01	44.07	41.68	63.78	60.33
		45.11		65.69		42.93		62.38	
Choline-N-methyl-C^{14} Starved Animals	1	5.96		13.81		3.62		7.96	
Lactate-3-C^{14} Starved Animals	3	49.90		63.81		49.01		65.39	
		59.48	54.35	74.84	70.32	53.82	53.06	68.82	68.92
		53.67		72.32		56.36		72.55	

Experimental and Results. Long-Evans female rats weighing between 180 and 200 g. were injected intraperitoneally with 10 mg. (100 μc.) $C^{14}H_3COONa$. Either one or two hours later the rats were sacrificed by ether anaesthesia and blood obtained by heart puncture, using a syringe and needle previously rinsed with 1 percent sodium citrate solution. In general, about 5 cc. of blood were obtained from each rat. The blood was allowed to clot at room temperature for about two hours and then the serum and red cells were separated by centrifugation. The activity of each fraction was determined by direct plating, the red cells having first been suspended in saline. A windowless flow Geiger counter and platinum plates were used for all activity determinations. The plates were counted, acidified with acetic acid, dried and recounted. Activity loss was assumed to be due to volatile acetate metabolites in the blood. Serum samples lost an average of 15 percent of their activity as volatile acids. Loss from red blood cells was negligible. Non-volatile activity per ml. of the serum amounted to 0.12-0.15 percent of the injected dose. Red blood cells contained an average of 0.05 percent of the injected activity per ml. of cells. This was true whether animals were sacrificed one or two hours after injection.

Aliquot portions of serum samples were separated into protein, phospholipid, fatty acid, non-saponifiable and glycerol fractions. The activity of each fraction was determined by direct plating. Separation of various fractions was effected by the following scheme (Table 13) which is essentially the same method as that reported by Kritchevsky and Kirk. (D. Kritchevsky and M. Kirk, "Radioactive Eggs. II. Distribution of Radioactivity in the Yolks", Proc. Soc. Exptl. Biol. Med., 1951, 78, 200-202.) The results obtained on the activity in the various serum fractions is shown in Table 14.

Conclusions. The level of activity in the blood after injection of sodium acetate-2-C^{14} remains fairly constant at least for the first two hours, in spite of the fact that approximately 65-70 percent of the activity has been exhaled as $C^{14}O_2$.

Although no explanation of the differences between blood from heparinized and non-heparinized animals is immediately apparent, these differences are great enough to warrant further investigation.

TABLE 13

Scheme for Separating Blood Serum into Various Fractions

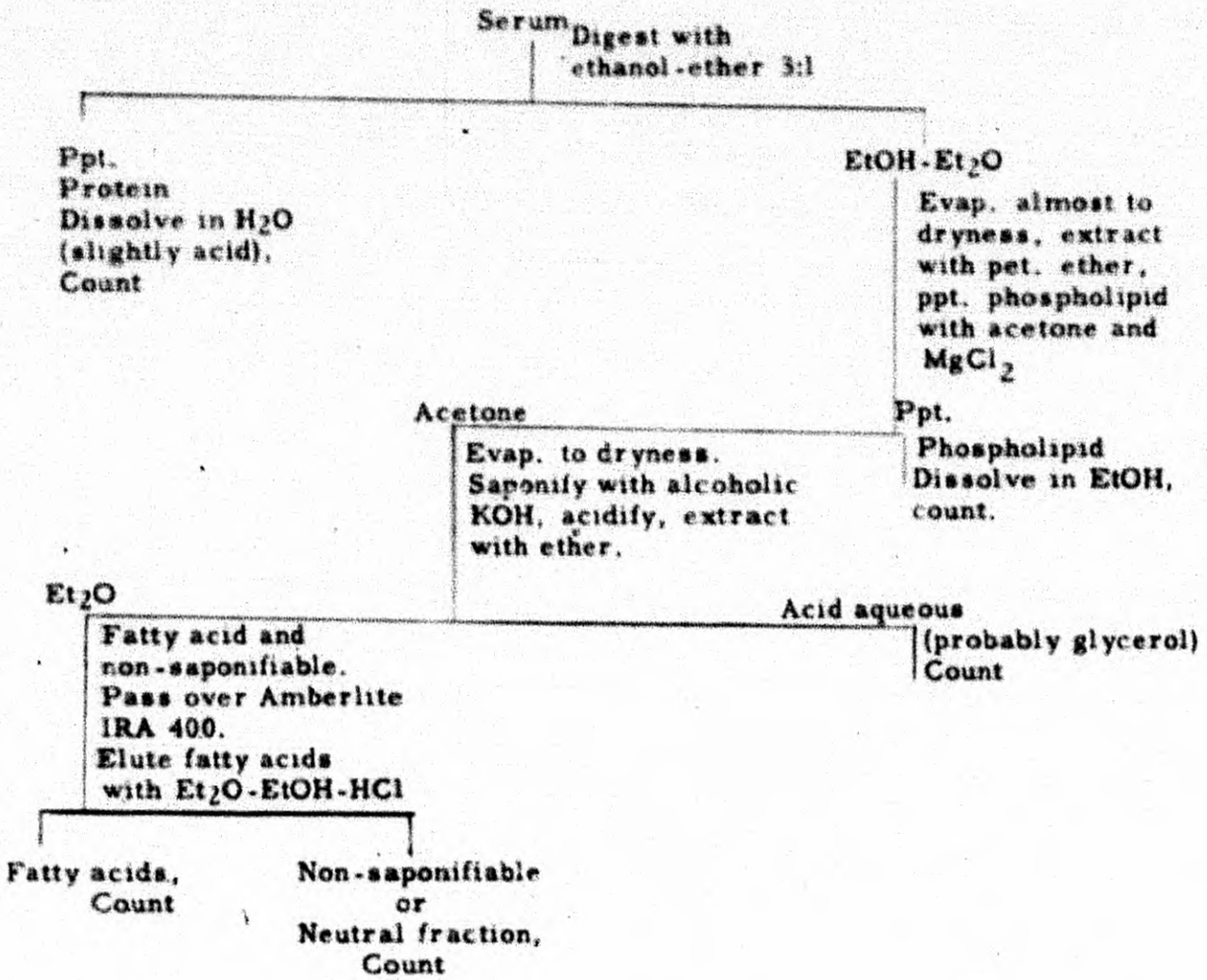

TABLE 14

Average % of the Activity of the Starting Serum Found in Each Fraction

Fraction	Acetate only	Acetate and heparin
Protein	93.0%	93.9%
Phospholipid	1.10	0.73
Fatty Acid	1.15	2.07
Non-saponifiable (sterols)	1.41	3.92
Acid aqueous (probably glycerol)	2.23	0.59

Δ^7-Cholestenol Content of Serum Cholesterol

R. M. Lemmon and Margaret Anderson

More than 100 g. of Δ^7-cholestenol ("lathosterol") have been synthesized from cholesterol by means of the synthetic procedure outlined in our previous report. The product has been identified by its melting point, ultra-violet spectrum, infra-red spectrum, and carbon and hydrogen analysis. These same data have also been obtained for the acetate and benzoate esters of lathosterol and they are all in good agreement with the values reported in the literature. Initially we had considerable difficulty in obtaining satisfactory carbon analyses for the product and for its acetate ester (the benzoate ester always gave good carbon analyses). However after several recrystallizations, both from methanol and from acetone, we were able to obtain products which gave very satisfactory carbon and hydrogen analyses.

We are now ready to begin an animal feeding program with the lathosterol. This work will be carried on in collaboration with the Medical Physics Group. The principal aims of the feeding program will be to determine if the presence of the lathosterol in the diet will have any effect in retarding the appearance of atherosclerosis or in promoting its disappearance. Particular attention will be made to any effect of lathosterol on the serum lipoproteins in the S_f 10-30 molecular weight group.

A Possible Primary Quantum Conversion Act of Photosynthesis

M. Calvin and J. A. Barltrop

To account for the observation[1, 2, 3] that illumination prevents the appearance of newly assimilated carbon in the compounds of the tricarboxylic acid cycle, it was suggested[3] that the light shifts the steady-state condition of the thioctic acid-containing coenzyme[4, 5] (protogen, lipoic acid, thioctic acid, P.O.F.) toward the reduced (dithiol) form, in which condition it is incapable of oxidatively decarboxylating pyruvic acid,[6, 7] newly formed from CO_2, to give rise to the acetyl-CoA[8, 9, 10] required to bring this carbon into the compounds of the Krebs cycle. We are here reporting some observations leading to the further suggestion that this shift toward the dithiol form is the direct result of the light action and that a bi-radical formed by dissociation of the disulfide bond in a strained five-membered disulfide containing ring (as in 6,8-thioctic acid and trimethylenedisulfide) is the species in which the quantum absorbed by the plant pigments and stored as electronic excitation in chlorophyll[11] appears first as chemical bond potential energy, i.e., that a possible primary quantum conversion act of photosynthesis is represented by the equation

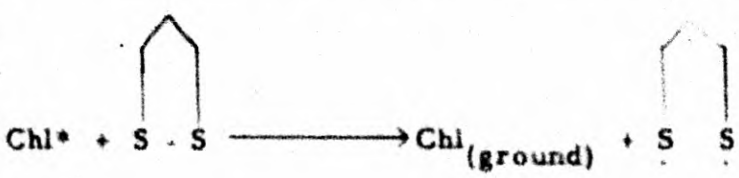

(I)

Subsequent abstraction of H atoms[12,13] from a suitable donor by the three free radicals would lead to the diphenyl which would be recaptured ultimately by CO_2. The residual oxidation product of the H donor would lead in the end to molecular oxygen. It is obvious that on both the reductant and oxidant sides the chemical products of the conversion of several quanta will be required to accomplish the reduction of each CO_2 molecule and the generation of each O_2 molecule.

These subsequent reactions, being strictly chemical, may lead to diverse energy rearrangements. For example, the chemical potential of reduced carbon might be converted by oxidative phosphorylation reactions into the energy of phosphoric anhydrides, which in turn, could raise the potential energy of intermediates in the reaction sequences leading to the evolution of molecular oxygen and the reduction of CO_2.[14,15]

A value of the dissociation energy for this particular disulfide lying in the region of 30-40 Kcals would constitute not only permissive evidence for reaction (1) but positive evidence in its support, since hitherto it has been difficult to suggest any likely primary chemical step capable of usefully absorbing the greater part of the 30-40 Kcal quantum of electronic excitation available for photosynthesis. Estimates of D(RS-SR) from simple open chain compounds range from 50[16] to 70[17] Kcals. However, the fact that 6,8-thioctic acid is colorless, while 6,8-thioctic acid is yellow,[18] suggested that the incorporation of the S-S bond into a 5-membered ring might indeed introduce sufficient strain into it so as to reduce the S-S dissociation energy by as much as 25-30 Kcals., thus bringing it down into the required range. A number of experiments have been performed using the product of the reaction of Na_2S_2 with $(CH_2)_3Br_2$ (trimethylenedisulfide) as a model substance. Its absorption spectrum, together with that of the two thioctic acids and n-propyl disulfide is shown in Fig. 5. Estimates of the dissociation energy of the S-S bond in the trimethylenedisulfide were obtained from measurements of the rate of fading (at ca. 80°C.) of the colored radical diphenylpicrylhydrazyl in petroleum ether in the presence of $(CH_2)_3S_2$, and of the rate of pyrolysis of the disulfide in octane at elevated temperatures. Both processes appeared to obey unimolecular kinetics and the derived free energies of activation were found to be respectively ca. 27 Kcals. and 35 Kcals. Furthermore, it was found that a photochemical polymerization of the disulfide by light of wave length greater than 4,000 Å was sensitized by zinc tetraphenylporphyrin. Also, a light-induced fading of diphenylpicrylhydrazyl at room temperature and dependent on the presence of the disulfide has been demonstrated. These results may be taken to indicate that the dissociation energy of the disulfide bond is in fact in the range 25-35 Kcals. and that this dissociation may be brought about by energy transfer from some other molecule in a suitably excited state.

That such energy transfers may take place, and especially efficiently in condensed systems, has been amply demonstrated.[20,21,22,23,24] Since the grana have the optical properties of a condensed chlorophyll phase,[25,26,27,28] a quantum absorbed anywhere within that phase is very rapidly transferred among the identical molecules of that phase at the singlet or the triplet levels. Concomitant with this, there occurs a decrease in the probability of emission as fluorescence[20,21,22,29] and hence an increase in the availability of the quantum for chemical transformation (disulfide fission). In such a system, the high efficiency of energy conversion may be retained even though the ratio of chlorophyll to disulfide molecules be large (10^2-10^3).

References

1. A. A. Benson and M. Calvin, J. Exptl. Bot., 1, 63 (1950).

2. J. W. Weigl, P. M. Warrington and M. Calvin, J. Am. Chem. Soc., 73, 5058 (1951).

3. M. Calvin and Peter Massini, Experientia, in press.

4. G. W. Kidder and V. C. Dewey, Protozoa, I, 388, Academic Press (1951).

5. E. L. Patterson, J. A. Brockman, Jr., F. P. Day, J. V. Pierce, M. E. Macchi, C. E. Hoffman, C. T. O. Long, E. L. R. Stokstad and T. H. Jukes, J. Am. Chem. Soc., 73, 5919 (1951).

6. L. J. Reed, B. D. DeBusk, I. C. Gunsalus and G. H. F. Schnakenberg, J. Am. Chem. Soc., 73, 5920 (1951).

7. I. C. Gunsalus, L. Struglia and D. J. O'Kane, J. Biol. Chem., 194, 859 (1952).

8. J. R. Stern, Phosphorus Metabolism, I, Johns Hopkins Press (1951).

9. S. Korkes, Phosphorus Metabolism, I, Johns Hopkins Press (1951).

10. R. S. Schweet, M. Fuld, K. Cheslock and M. H. Paul, Phosphorus Metabolism, I, Johns Hopkins Press (1951).

11. L. N. M. Duysens, Nature, 168, 548 (1951).

12. A. F. Bickel and E. C. Kooijman, Nature, 170, 211 (1952).

13. E. F. P. Harris and W. A. Waters, Nature, 170, 212 (1952).

14. Phosphorus Metabolism, I, Johns Hopkins Press (1951), Section V.

15. M. Calvin, J. A. Bassham, A. A. Benson and P. Massini, Ann. Rev. Phys. Chem., 3, 215 (1952).

16. A. H. Sehon, J. Am. Chem. Soc., 74, 4723 (1952).

17. J. L. Franklin and H. E. Lumpkin, J. Am. Chem. Soc., 74, 1024 (1952).

18. Several milligrams of each of these synthetic[19] products were obtained through the courtesy of Dr. T. H. Jukes of Lederle Laboratories.

19. M. W. Bullock, J. A. Brockman, Jr., E. L. Patterson, J. V. Pierce and E. L. R. Stokstad, J. Am. Chem. Soc., 74, 3455 (1952).

20. H. Kallman and M. Furst, Phys. Rev., 79, 857 (1950).

21. H. Kallman and M. Furst, Phys. Rev., 81, 853 (1951).

22. H. Kallman and M. Furst, Phys. Rev., 85, 816 (1952).

23. M. M. Moodie and C. Reid, J. Chem. Phys., 20, 1510 (1952).

24. C. Reid, Phys. Rev., 88, 422 (1952).

25. S. Granick and K. R. Porter, Amer. J. Bot., 34, 545 (1947).

26. M. Calvin and V. Lynch, Nature, 169, 455 (1952).

27. E. E. Jacobs and A. S. Holt, J. Chem. Phys., 20, 1326 (1952).

28. A. Frey-Wyssling and K. Mühlethaler, Vierteljahrsschrift der Naturf. Ges. Zurich, 94, 182 (1949).

29. D. McClure, private communication.

30. We are indebted to Mr. Paul Hayes for the determination of these absorption spectra.

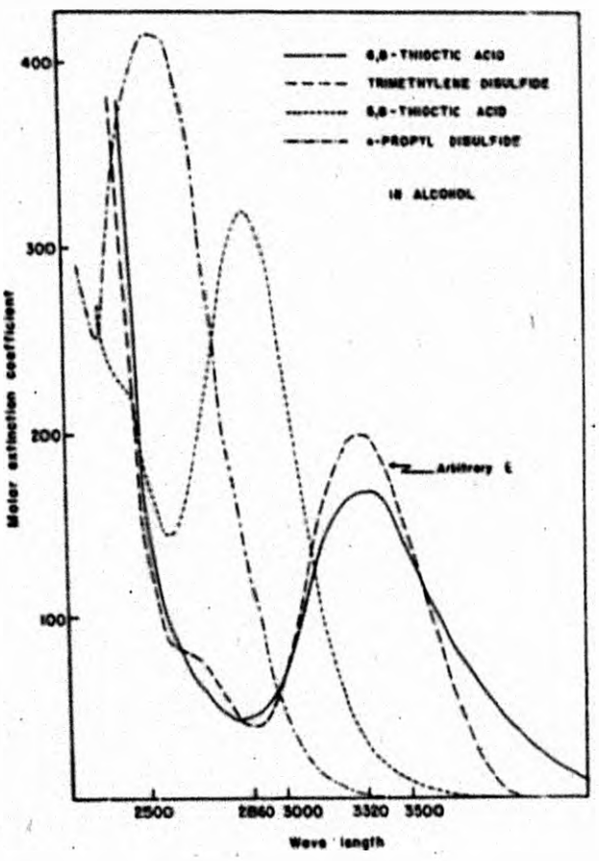
6,8-THIOCTIC ACID
TRIMETHYLENE DISULFIDE
6,8-THIOCTIC ACID
n-PROPYL DISULFIDE
IN ALCOHOL
Arbitrary ε
Molar extinction coefficient
400
300
200
100
2500
2860
3000
3320
3500
Wave length

Fig. 5

Short-Time Photosynthesis Experiments: Sugar Degradations

L. Daus and A. Harris

Short Time Soy Bean Leaf Photosynthesis Series and Sedoheptulose Degradations

A series of photosynthetic experiments was performed on soy bean leaves with samples taken at 0.75, 1.5, 3.5 and 5 seconds. Another experiment was done with semi-automatic introduction of CO_2 and subsequent alcohol killing which was timed at 0.4 seconds. The general distribution of radioactivity among resulting compounds was determined by counting the chromatographed extract directly on the paper. The distribution of radioactivity in sedoheptulose was investigated with periodate degradations of sedoheptulosan and of sedoheptulosazone, giving, respectively, percentages of the total activity in carbon 4, and in carbons 7, 1+2+3, and 4+5+6. The data obtained corresponded quite well with that from previous experiments with soy bean leaves and all of these available data are tabulated in Table 15. Degradations on the 0.4 second experiment are still in progress. In evaluating the data, it must be remembered that at such short times the error in timing is large, and that any delays in inactivation of the enzyme systems by the boiling alcohol become increasingly important.

The most noteworthy information obtained from the general distribution of radioactivity in these short time experiments seems to be in the increasing predominance of phosphoglyceric acid as time approaches zero, and the decreasing of the "hexose monophosphate area" (mostly fructose and sedoheptulose phosphates) from 61 percent of fixed activity in 20 seconds to only 3 percent in 0.4 seconds. In addition, in times up to 5 seconds, the activity not in the glyceric acid or hexose monophosphate area appeared mainly in the pentose phosphate, triose phosphate and phosphopyruvate areas; in the 0.4 second experiment, this activity about equaled the activity in the hexose monophosphate area and at longer times it was much less than the hexose monophosphate activity. Of further interest is the fact that in the shortest experiments (0.4 seconds, 0.75 seconds) the amounts of free fructose and sedoheptulose were almost equal; in 5 minutes there is almost twice as much label in sedoheptulose as in fructose.

Degradation data indicate that the percentage of activity in carbon 4 of sedoheptulose rises from a low value at zero time to a maximum of about 30 percent and then drops to 14 percent (the value for uniform labeling). Degradation of sedoheptulosan from the 0.4 second experiment will be a check on this apparent trend. The information from degradation of 0.75 second sedoheptulosazone indicates that even at this short a time there are at least three highly labeled atoms: 4; 5 and/or 6; and 1 and/or 2 and/or 3. Carbon 7 has very little activity in this short time. There is a good probability that carbon 6 is also low, which would mean 5 increases at shorter times. The fructose from the 0.75 second experiment was degraded with the following results: 1+2+3 = 47.8 percent; 4+5 = 50.5 percent; 6 = too low to count.

TABLE 15

General Distribution	0.4 Sec.	0.75 Sec.*	1.5 Sec.*	3.5 Sec.*	5 Sec.*	6-8 Sec.**	6 Sec.	10 Sec.	15 Sec.***	20 Sec.	5 Min.
%of total in PGA + free glyceric acid	93.0	85.0	58	63	51	37	22.0			19.0	2.1
%of total in HMP	3.1	14.0	41	31	41	53	51.0			61.0	12.0
Relative amts. of following cpds. - determined after hydrolysis											
Glyceric acid	95.0	85.0	58	65	56	40					
Fructose	1.4	7.0	18	13	16	17	1.0			1.0	1.0
Sedoheptulose	1.7	7.5	23	18	26	33					1.9
Glucose	0	0	0	2	2	10	0.9			1.3	2.0
Distribution in the Carbon Chain of Sedoheptulose Carbon No.											if=distrib.
4		18.0	24	26	29	24	24.0	28	24	21.0	14 14
1+2+3	43.0				36				41	44.0	43.0
4+5+6	60.0				64				53	--	43.0
7	2.0				2				5	5.0	14.0

* Experiments performed at one time
** Part of leaf killed at 6 seconds, the rest not until about 8 seconds
*** Data from B. W. Racusen and S. Aronoff, Archives of Biochemistry and Biophysics, in press.

In hopes of obtaining values for the activity in carbon 1, the reaction of lead tetraacetate on ketoses is being investigated. This reaction should give the two terminal atoms as formaldehyde and the center carbons as CO_2. Conditions have been found using carrier glucose and uniformly labeled fructose to give in two experiments, 30 percent and 32 percent for formaldehyde and 75.5 percent and 70.5 percent for CO_2 (theoretical would be 33 percent and 67 percent respectively). The reaction will now be tested on uniformly labeled sedoheptulose and then, if it proves practical, used on sedoheptulose from the series of soy bean experiments.

The sedoheptulosan from 5 seconds photosynthesis Scenedesmus (see below for ribulose degradations) was degraded to give 17.5 percent of the activity in carbon 4.

Degradation of Ribulose

The degradation of ribulose by periodate oxidation of the osazone (using a rabinose carrier) has been continued. A degradation of ribulose from a 5 second photosynthetic Scenedesmus experiment gave the results shown in Table 16.

TABLE 16

Carbon Atoms	Compound Isolated	%Activity
1, 2, 3	1, 2 bisphenyl-hydrazone	95.0 ± 9
4	Barium formate	2.5 ± 3
5	Formaldimedon	1.8 ± 3

Direct periodate oxidation of ribulose as previously reported (Quarterly Report for July, August, September, 1951) gives a fairly good indication of the distribution of activity in carbons 3 and 4 together, providing the ribulose sample is not contaminated with ribose. The latter degradation was performed on ribulose from the previously mentioned 5 second Scenedesmus experiment. In this degradation, 71 percent of the activity was found in carbons 3 and 4. Since carbons 4 and 5 appear to be equally labeled, as evidenced by several osazone degradations, carbon 3 can be calculated by subtracting the value for carbon 5 (= carbon 4) from that of the total of 3 + 4. Table 17 summarizes the results.

TABLE 17

Distribution of Radioactivity in Ribulose

Carbon Atom	Time of Photosynthesis 5 sec.	30 sec.	60 sec.	2.5 min.
3 + 4	71	52	44	37
5	2	6	11	18
3 (if 4 = 5)	68	46	33	19

Further attempts to degrade the 1, 2 bisphenyl-hydrazone of mesoxaldehyde have been continued. An attempted preparation of the osatriazole from the aldehyde by refluxing with $CuSO_4 \cdot 5H_2O$ resulted in the formation of 4-benzalozo-1-phenylpyrazole.

A cyclic thioacetal of the aldehyde (m.p. 195-6°) has been prepared from 1, 2-ethanedithiol. It is hoped that this compound will prove to be a useful intermediate in proposed degradations of the aldehyde, for example: (1) oxidation to a disulfone by monoperphthalic acid and subsequent hydrolysis, or (2) hydrolysis of the hydrazone groups and periodate oxidation of the resulting dicarbonyl compound.

Mathematical Models of Biological Systems

D. Bradley

Experiments on the path of carbon in photosynthesis have led us to postulate a sequence of reactions by which carbon dioxide is transformed into intermediary metabolites with complex carbon skeletons. The chain of reasoning from experimental observations to postulated sequence, however, has been neither logically consistent nor quantitative because of the complexity of the system under observation. Because of this lack of logical consistency it is possible that some of the available experimental details may contradict either qualitatively or quantitatively predictions based on the proposed scheme. However, the complexity of the scheme has in the past precluded the deduction of such quantitative predictions. Recently we have set up a mathematical model of a biological system which when coupled with a proposed scheme permits calculation of observable parameters. These are compared with experimental results ard the validity of the scheme is evaluated on the basis of agreement or lack of it.

We assume that there exist within the plant metabolic pools or reservoirs, meaning merely that any newly formed member of a particular molecular species mixes completely with a definite amount of the species before reacting further. This "definite amount" is called the reservoir size, R, of that species. In practice, though no in principle, we must also assume that isotope effects on the reactions are trivial. With these assumptions we may set up a differential equation for the appearance of radioactivity in any intermediate, A. Consider the model set of reactions, Fig. 6, (under "steady state" conditions),

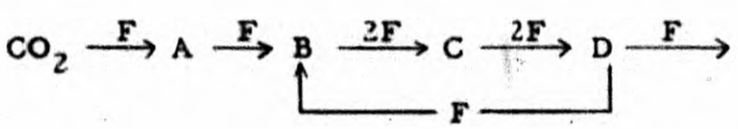

Fig. 6

where A, B, C, D are intermediates in CO_2 fixation, F is the fixation rate of CO_2 of specific activity one. The rate of change of activity, a, in A is

$$\frac{da_A}{dt} = \text{rate of incorporation of radioactivity - rate of loss through reaction to B}$$

$$= F - F \cdot X_A$$

where X_A is the specific activity of A. Substituting $a_A = R_A \cdot X_A$

$$\frac{dX_A}{dt} = \frac{F}{R_A}(1 - X_A)$$

this differential equation may be solved for X_A handily if

$$\frac{d\left(\frac{F}{R}\right)}{dt} = 0$$

which corresponds to steady state experimental conditions (M. Calvin and P. Massini, Experientia, in press). In a similar fashion an equation may be set up for any intermediate, for example, B,

$$\frac{dX_B}{dt} = \frac{F}{R_B}(X_D + X_A - 2X_B)$$

In practice one equation must be set up for each carbon atom of each compound in the sequence into which radioactivity is incorporated. Using the single experimental parameter (F/R) for each atom as determined from very long experiments (Calvin and Massini), in conjunction with our proposed "photosynthetic cycle" we may set up the differential equations for the rate of appearance of radioactivity in every atom of every compound in the cycle. We can compare these predictions with experimental total activity appearance curves for compounds and intra-compound distribution of radioactivity from degradation studies.

The chief practical limitation on this technique is in the integration of the differential equations. A typical cycle of interest is shown in Fig. 7, in which a two-carbon compound is carboxylated to form PGA (phosphoglyceric acid) which is reduced to phosphodihydroxyacetone, which forms both hexose and, by a subsequent carboxylation and condensation, a sedoheptulose phosphate

which splits to a two-carbon acceptor compound and a ribulose phosphate which splits to another two-carbon acceptor compound plus triose. In the cycle, only carbon skeleton changes are considered, and lines between atoms represent the fate of an atom during a reaction. F, 2F, etc. (over the lines) represent the relative reaction rates. There are eighteen differential equations for this simple cycle, many of them simultaneous. The difficult integration was performed by the UCRL differential analyzer. In Fig. 8 are calculated degradation curves for phosphoglyceric acid in this cycle (white circles). The time scale is inversely proportional to the fixation rate which was taken from the paper by Calvin and Massini. The black points represent the degradation data of Fager, Rosenberg and Gaffron (Federation Proc., 9, 535 (1950)) who used the same organism, Scenedesmus, and using the additional relationship that α-carbon activity = β-carbon activity (this equality is indicated by degradation data obtained in this laboratory). As these authors published no total fixation rate data on the series, we adjusted the time scale by making their 60-second point fit the curve at 20.6 seconds and multiplying all their other four times by 20.6/60. The agreement is satisfactory but unfortunately several other proposed schemes also exhibit the same degree of agreement and at present we are unable to pick a unique scheme from the data available. We are now awaiting degradation data in this laboratory on sedoheptulose and ribulose as functions of time to compare with the various proposed schemes.

The integrations are tedious, requiring almost a full day's use of the differential analyzer for a single cycle with one set of (F/R) parameters. This obviously seriously limits our ability to determine the effects of small changes in schemes on the predicted results. Work is in progress to determine the feasibility of constructing an RC integrating circuit which could complete an integration in a matter of a few minutes. Such an instrument would greatly facilitate the extension of this work, not only in the path of carbon in photosynthesis but phosphate, sulfate and other assimilation processes in biology.

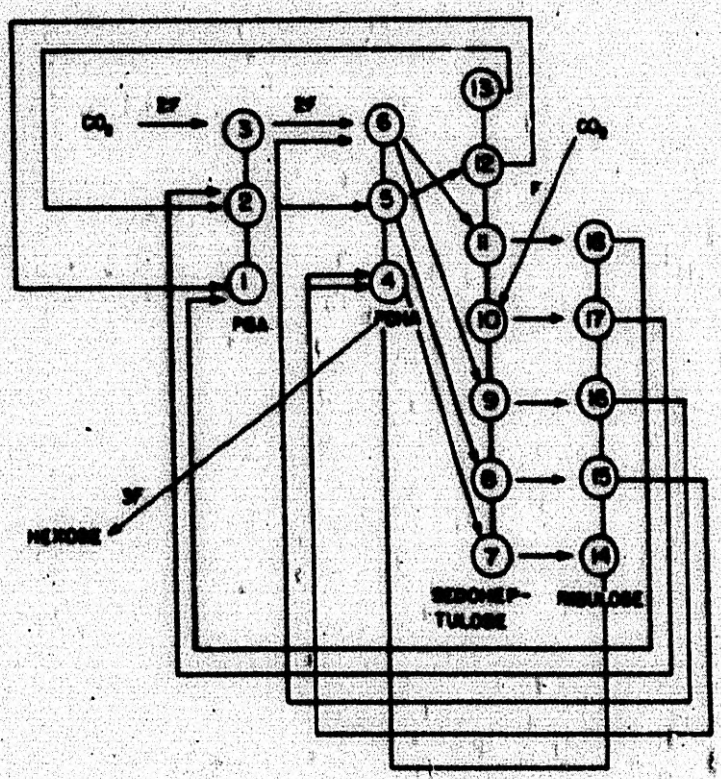
CO_2
3P
3P
3
6
13
12
CO_2
2
5
11
16
1
4
10
17
PGA
PGA
9
18
3P
HEXOSE
8
15
7
14
SEDOHEP-
TULOSE
RIBULOSE

FIG. 7

MU-4744

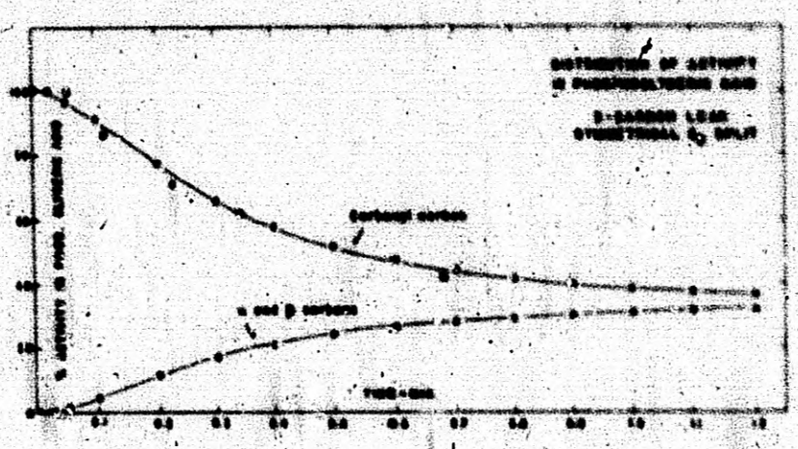

Fig. 8

II. QUARTERLY PROGRESS REPORT. Project 48B

W. M. Latimer, Director

A. Metals and High Temperature Thermodynamics

Leo Brewer, LeRoy Bromley, Albert Rothman,
Richard Porter, Oscar Krikorian and James Kane

Refractory Silicides

The study of the reaction of refractory silicides with carbon and nitrogen has been completed. The results have allowed the fixing of the relative stabilities of the silicides. Limits have been set to the heats of formation of the silicide phases.

Molybdenum Chlorides

An apparatus has been constructed to restudy the molybdenum chloride gaseous molecules. Previous studies had indicated $MoCl_4$ to be an important molecule at high temperatures. However the data gave an entropy value that was quite unreasonable. Preliminary work with the new apparatus indicates that the previous work was in error due to the presence of small amounts of water which form a very stable oxy-chloride molecule.

Alkaline Earth Oxide Gases

The spectrum of MgO has been observed in emission using MgO in the King furnace. It is planned to observe this emission as a function of temperature to determine the heat of formation of the MgO gaseous molecule. YO, VO, MgH, and TiO have also been observed in the King furnace.

Carbon Fluorides

A new molecule believed to be C_2F_2 was reported previously. Further studies show that this molecule cannot be prepared below 1600° C, but the action of graphite upon CF_4 at higher temperatures does form this new molecule which can then be cooled to lower temperatures where its rate of decomposition is low.

Review of Thermodynamic Data for Oxide Systems

A comprehensive review of the phase relations of oxide systems, the thermodynamic data of the various phases, and the stabilities of the gaseous molecules has been completed and is scheduled to be published in the February issue of Chemical Reviews.

Thermal Conductivity of Gases at High Temperatures

Several constructional difficulties have delayed the completion of the thermal conductivity cell. The furnace was completed, but a short circuit during a trial warm-up necessitated rebuilding the furnace core and winding. Both of these items should be repaired shortly. Report UCRL-1852 has been issued. The regulators and power supply have been constructed and await testing.

The chief work remaining now consists of setting up the gas-filling and vacuum supply, setting up the measuring equipment, calibrating the thermocouples, and providing constant heating sources.

B. Basic Chemistry, Including Metal Chelates

R. E. Connick, William Jolly, Albin Zielen, Frank Owings, Howard Mel, Lorin Hepler and John Kury

Studies Involving Liquid Ammonia as a Solvent

A Beckman glass electrode and a Beckman calomel electrode were modified for use in liquid ammonia at -33° C. The aqueous cell solutions were replaced with ethanolic solutions. However, the potential across these two electrodes in liquid ammonia did not appear to be affected by tremendous changes in the hydrogen ion concentration in the ammonia, even though the electrodes functioned nicely in aqueous solutions. The hope of using a glass electrode in ammonia has been temporarily abandoned.

An attempt is being made to measure the vapor pressure lowering of dilute salt solutions in liquid ammonia at 25° C. A differential method is being employed, using liquid ammonia as the manometric fluid. By this means it would be possible (with adequate temperature control) to measure easily vapor pressure lowerings of the order of several parts in a million. But adequate thermostating of the simple glass apparatus is apparently very difficult, and results so far have been erratic and only good to ± 0.01 percent in P/po.

In a previous tabulation of heats, free energies and entropies in liquid ammonia (cf. UCRL-1402), many free energies based on solubilities are undoubtedly in error because of the assumption that the solid phases in contact with the saturated solutions are unsolvated.

Even though analytical data on solid phases in liquid ammonia solubility studies are lacking, it is possible, by searching the literature for vapor pressure data on solid ammonates, to ascertain the nature of the solid phases. The recalculation of the free energies is in progress.

Thermodynamics of Indium

The work on the complexing of indium by fluoride has been completed at 15°, 25°, and 35°. Thermodynamic constants for the following equilibria have been determined at all three temperatures.

$$In^{+3} + HF = InF^{++} + H^{+}$$

$$InF^{++} + HF = InF_2 + H^{+}$$

The results of this work will be published shortly.

In connection with this work on indium-fluoride complex ions the ferric-fluoride couples ions were also investigated.

Experiments designed to investigate the equilibria between $In_{(m)}$, In^{+}, In^{+2}, and In^{+3} by the method previously reported are in progress. Definite indication of the existence of at least one of the lower oxidation state species has been observed. It is hoped that the equilibria between the various oxidation states can be measured. Experiments to this end are being carried out.

Ferric Fluoride Complex Ions

The extent of complexing of ferric ion by fluoride ion was measured. The method used has been described previously.

Experiments were carried out at an ionic strength of 0.5. The equilibria in question are:

$$Fe^{+++} + HF = FeF^{+2} + H^{+} \qquad K_1$$

$$FeF^{+2} + HF = FeF_2^{+} + H^{+} \qquad K_2$$

$$FeF_2^{+} + HF = FeF_3 + H^{+} \qquad K_3$$

The values obtained at 25° C for the equilibrium quotients are:

$$K_1 = 184$$
$$K_2 = 10.3$$
$$K_3 = 1.0$$

The Hydrolytic Polymerization of Zirconium

Work is proceeding on the determination of the molar extinction coefficient at the 3660 Å peak of the first Zr - TTA (thenoyltrifluoracetone) complex in 2M $HClO_4$ solutions. The concentration of the Zr complex species is obtained by means of the known molar extinction coefficients of TTA plus

the decrease in the solution's optical density, due to added zirconium at the TTA peaks of 2920 and 2665 Å.

Simultaneously data are obtained that will allow a second calculation of the molar extinction coefficient by the method employed by McVey (HW-21487) in his work in 4 M $HClO_4$.

Thermodynamics of Sulfide Ion

Proper evaluation of thermal data for $S^=$ requires a knowledge of the second acid dissociation constant of H_2S. Recent investigations by Kubli[1] and Konopik and Leberl[2] indicate that this constant is now known with reasonable accuracy.

Hence a series of calorimeter experiments on the heat of neutralization of H_2S solutions by NaOH at 25° C is now being carried out. The relative concentrations of HS^- and $S^=$ are controlled by the amount of NaOH added.

This thermal data in conjunction with the foremention equilibrium constant will be used to calculate heats of formation and partial molal entropies of $S^=$ and HS^-.

Potential of the RuO_4^- - RuO_4 Couple

Experiments on the reaction of ClO_2^- with RuO_4^- and $RuO_4^=$ in alkaline solution, have shown that a steady state in ruthenium is established, which can be explained in terms of the following mechanisms:

I. (1) $ClO_2^- + H_2O \overset{K_{hI}}{=} HClO_2 + OH^-$

(2) $RuO_4^= + HClO_2 \xrightarrow[k_I]{r.d.} RuO_4 + ClO^- + OH^-$

(3) $ClO^- + H_2O = HClO + OH^-$

(4) $RuO_4^= + HClO \xrightarrow{rapid} RuO_4 + Cl^- + OH^-$

(5) $2\left[RuO_4 + RuO_4^= \xrightarrow{rapid} 2\,RuO_4^-\right]$

---

(6) $4RuO_4^= + ClO_2^- + 2H_2O \longrightarrow 4RuO_4^- + Cl^- + 4OH^-$

$-d(RuO_4^=)/dt = 4\,k_I(RuO_4^=)(HClO_2) = 4k_IK_{hI}(RuO_4^=)(ClO_2^-)/(OH^-)$

---

1. H. Kubli, Helv. Chem. Acta., 29, 1962 (1946).
2. N. Konopik and O. Leberl, Mh. Chem., 80, 781 (1949).

II. (1) $2\ RuO_4^- \overset{K}{\rightleftharpoons} RuO_4 + RuO_4^=$

(2) $RuO_4 + ClO_2^- \xrightarrow[k_{II}]{r.d.} RuO_4^= + ClO_2^+$

(3) $ClO_2^+ + OH^- \xrightarrow{rapid} HClO_3$

(4) $HClO_3 + OH^- \xrightarrow{rapid} ClO_3^- + H_2O$

---

(5) $2RuO_4^- + ClO_2^- + 2OH^- \longrightarrow 2RuO_4^= + ClO_3^- + H_2O$

$$+ d(RuO_4^=)/dt = 2k_{II}(RuO_4)(ClO_2^-) = 2k_{II}K\frac{(RuO_4^-)^2}{(RuO_4^=)}(ClO_2^-)$$

The constant $k_I K_{hI}$ was obtained from rate data, and K_{II} calculated from steady state data and a value for K based on an approximate potential of -0.97 volts for the RuO_4^- - RuO_4 couple.

These results have been used to explain a similar steady state in ruthenium occurring in the oxidation of perruthenate by hypochlorite, by means of the following mechanisms:

III. (1) $2\ RuO_4^- \overset{K}{\rightleftharpoons} RuO_4 + RuO_4^=$

(2) $ClO^- + H_2O \overset{K_{hIII}}{\rightleftharpoons} HClO + OH^-$

(3) $RuO_4^= + HClO \xrightarrow[k_{III}]{r.d.} RuO_4 + Cl^- + OH^-$

---

(4) $2RuO_4^- + ClO^- + H_2O \longrightarrow 2RuO_4 + Cl^- + 2OH^-$

$$+ d(RuO_4)/dt = 2\,k_{III}(RuO_4^=)(HClO) =$$

$$2k_{III}K_{hIII}K\frac{(RuO_4^-)^2(ClO^-)}{(RuO_4)(OH^-)}$$

IV. (1) $RuO_4 + ClO^- + OH^- \xrightarrow[k_{IV}]{r.d.} RuO_4^= + HClO_2$

(2) $HClO_2 + OH^- \xrightarrow{rapid} ClO_2^- + H_2O$

(3) $RuO_4 + ClO_2^- \xrightarrow{rapid} RuO_4^= + ClO_2^+$

(4) $ClO_2^+ + OH^- \xrightarrow{rapid} HClO_3$

(5) $HClO_3 + OH^- \xrightarrow{rapid} ClO_3^- + H_2O$

(6) $2[RuO_4^= + RuO_4 \xrightarrow{rapid} 2RuO_4^-]$

---

(7) $4RuO_4 + ClO^- + 4OH^- \longrightarrow 4RuO_4^- + ClO_3^- + 2H_2O$

$$-d(RuO_4)/dt = 4k_{IV}\,(RuO_4)\,(ClO^-)(OH^-)$$

A value for k_{IV} was calculated from the equilibrium constant for reaction IV (1) (based on -0.97 volts for the RuO_4^- - RuO_4 potential) and the specific rate constant for the reverse reaction (k_I of reaction I (2)). k_{III} is known from direct rate measurements.

The calculated values of the steady state ratio $(RuO_4^-)/(RuO_4)$ agree with experiment within the limits of error of the measurements.

It is noteworthy that perruthenate appears to be relatively unreactive, oxidation or reduction occurring through the agency of the tetroxide or ruthenate respectively.

The (OH^-) dependence in some of the above reactions is not well established, and experiments to determine this dependence more reliably are in progress.

Study of Hydrates

Work continues on vacuum line preparation of $CaCl_2$ hydrates (September Quarterly); the heat of solution of a second sample of $CaCl_2 \cdot 2H_2O$ has been measured as 10.69 kcal/mole (c.f. 10.83 Kcal/mole on first determination). More consistent results are now being sought.

Thermodynamics of Thiosulfate

The value of the equilibrium constant for the reaction:

$$S_2O_3^{=}\ (aq.) + 2Ag(S) = SO_3^{=}\ (aq.) + Ag_2S(S)$$

has been determined as $K_c(123^oC) = 16.50 \pm 0.42$, using solutions of 0.2M concentration. The present work is on solutions at different concentrations at 123°C to determine K(123°C) at infinite dilution.

A new proportional temperature controller for the oil bath has been constructed and installed. The control element is a specially made 55 ohm platinum resistance thermometer operating in conjunction with an A. C. bridge, providing a potential temperature range of about 0-300° C. Any unbalance between the thermometer and bridge is fed into the grid of a 6AK5, subsequently amplified and combined with a phase change, thus operating a 2D21 thyratron for a longer or shorter priod of time. The 2D21 feeds into the primary of a 500 watt saturable reactor, the secondary of which operates a 250 watt control Calrod heater in the bath.

Bromate Thermodynamics

A start has been made on determining the heat of formation of BrO_3^- (aq.). At present, the calorimetric heat is inconsistent with the free energy and entropy data. Good agreement with the N.B.S. value has been obtained on two runs measuring the heat of solution of $KBrO_3$. An effort to obtain the heat of reduction of BrO_3^- to Br_2 by Br^- has proved calorimetrically unsuccessful. The reaction is too slow except at excessively high ionic strengths. The reduction of BrO_3^- is now being investigated using I^- on Fe^{++}.

C. Chemical Engineering (Process Chemistry) Section

D. N. Hanson, Director

Preparation of Titanium Metal. LeRoy Bromley and Alfred Petersen

The highest purity titanium metal is at present prepared by the Van Arkel-de Boer process in which a hot titanium filament is placed in an evacuated chamber containing crude titanium metal and a small amount of iodine. Iodine reacts with the crude titanium forming a volatile iodide which subsequently decomposes on the hot filament depositing pure metal.

A possible improvement in the method would be to immerse the hot filament in the liquid iodide. The filament temperature would be such that film boiling would result. By suitable choice of temperatures, pressures, reacting species, etc., it should be possible to improve thermal efficiency and also total cost.

TiI_4 was found to be available commerically at a prohibitive cost ($200/lb.). The procedure outlined by J. D. Fast (Rec. Trav. Chim. 58, 174 (1939) in which iodine is distilled and passed over the crude metal was tried but found to be not too effective.

Accordingly, excess Ti sponge and I_2 were mixed in a bulb flushed with argon and heated to melt the iodine. The bulb was equipped with a long open tube to allow pressure equilization and yet prevent I_2 from escaping. The exothermic reaction was at a moderate rate. The resulting product had the physical properties of TiI_4 and analyzed 96 percent TiI_4.

Film Boiling from Sub-Cooled Liquid. LeRoy Bromley and Eugene Motte

The apparatus to be used is that used for the forced convection film boiling studies reported in UCRL-1894 except for a few modifications.

A means of passing water and steam through the coils of the storage tank has been installed so that the liquid in the tank can be maintained at temperatures ranging from approximately 25° C to the boiling point of the liquid used. A new manometer has also been installed on the orifice below the storage tank. The apparatus has been cleaned and repaired as was deemed necessary for future operation.

It is proposed to measure the heat transfer to four liquids: ethyl alcohol, carbon tetrachloride, benzene, and hexane, and to correlate this data by the properties of the liquids, the velocity of the fluid, and the amount by which the liquids are sub-cooled below the boiling point.

Gas-Phase Mass Transfer Rates. Charles Wilke and Edward Lynch

Work has been completed on the first phase of this study and will be submitted in a final report in the near future.

Rates of mass transfer for the vaporization of water into air, helium, and Freon-12 were measured in a tower packed with one-inch Raschig rings. The "height of a transfer unit" was found to be a function of the inertia of the gas stream and the Schmidt number to the 0.47 power. Measurement of simultaneous heat and mass transfer with the wet-bulb thermometer supported the conclusion drawn above on the effect of Schmidt number.

The next phase of the problem will cover mass transfer in packed beds without liquid flowing.

Thermal Diffusion in the Liquid Phase. Charles Wilke and John Powers

This investigation had been under way since February, 1951, and was transferred to Radiation Laboratory in September, 1952, as a result of favorable progress.

The project has the purpose of investigating the operational variables involved in separation of liquids by thermal diffusion. Emphasis is being placed on continuous flow methods.

Design and construction of experimental equipment have been essentially completed It is planned to study first the ethyl alcohol-water mixtures, because fundamental thermodynamic data for the entire range of compositions are available in the literature. A preliminary run has been made and moderate revisions in the apparatus are being made to overcome the experimental difficulties that were encountered.

Multicomponent Phase-Equilibrium Measurements. Donald Hanson and Arturo Maimoni

The object of this investigation is the determination of liquid-vapor equilibria over a wide range of temperatures and pressures, 0-193 to 250° C and 0 to 2000 psig.

The following equipment is being assembled: a heavy stainless steel bomb containing the liquid phase is located inside of a thermostat. The vapor phase bubbles through the liquid and is recirculated until equilibrium is obtained. At this point liquid and vapor samples are obtained for subsequent analysis.

The present emphasis of the work is in development of a suitable sound interferometer to be used for composition analysis.

Capacity of Perforated Plate Liquid-Vapor Contacting Columns. Donald Hanson and Charles Hunt

The general program of this investigation covers the questions of vapor phase pressure drop, liquid entrainment, and plate instability with respect to dumping of liquid through perforations, but does not include any study of mass transfer rates or liquid flow problems. To date, work on pressure drop has included study of the following system variables: liquid height on plate, plate perforation diameter, perforation spacing, total area of perforations, gas density, gas viscosity, gas velocity.

The next phase of research will be concerned with the effect of liquid surface tension, liquid viscosity, and liquid density upon the pressure drop.

Mass-Transfer in Agitated Liquid Systems. Theodore Vermeulen and Homer Rea

Mass-transfer studies in agitated two-phase liquid systems related to solvent extraction and heterogeneous chemical reaction, have been retarded by an inability to specify the interfacial area available for mass transfer between the phases. This investigation was undertaken to study the effect of the physical properties of such a system on the formation of interfacial area, and on the resultant mass-transfer rates. A fully baffled tank was used under turbulent flow conditions.

CONFIDENTIAL

Interfacial areas have been determined by light transmission measurements through the unstable emulsion formed during agitation.

The effects of physical properties of the fluids, stirring speed, impeller geometry, and relative proportions of the two phases on interfacial area have been studied. No generalized correlation for all of these variables has yet been obtained. However it was found that for each system investigated

$$A = (\text{const.})\ 6\ \phi\ e^{-2\sqrt{\phi}}\ NL^{3/2}$$

where A = interfacial area, cm^2/cm^3, ϕ = volume fraction of disperse phase, N = stirring speed, L = impeller diameter, with a different value of the constant for each system. The power requirements for the agitation of two-phase systems were also investigated and were found to be identical with those for a homogeneous liquid of equal mean density. The study is being extended to measurement of mass-transfer rates in typical agitated systems.

Non-Aqueous Ion Exchange. E. Huffman and Theodore Vermeulen

The existing theories of column performance were used to interpret the breakthrough histories on solutions of amines in organic solvents, exchanging with Dowex 50 in the hydrogen form.

Slow rates of exchange were generally observed, and particle diffusion was found to be the controlling mechanism. The acid strength of the solvents, coupled with the low basicity of the amines, is proposed as the determining factor. If this interpretation is correct, the rates measured will apply only to the hydrogen cycle, and not to exchanges between readily dissociable ions. The rates that were measured corresponded to "thin bed" operation, and required a new extension of the calculation methods. It follows that, for non-aqueous hydrogen-cycle operations, the resin should be maintained in hydrated form wherever the organic solvent and process conditions will permit. These results were given fully in Report UCRL-1989.

CONFIDENTIAL

END